Turusov, V., Rakitsky, V., Tomatis, L., 2002. Dichlorodiphenyltrichloroethane (DDT): ubiquity, persistence, and risks. Environmental Health Perspectives 110, 125–128.

Wang, F., Roberts, S.M., Butfiloski, E.J., Morel, L., Sobel, E.S., 2007. Acceleration of autoimmunity by organochlorine pesticides: a comparison of splenic B-cell effects of chlordecone and estradiol in (NZBxNZW)F1 mice. Toxicological Sciences 99, 141–152.

Ward, M.H., Colt, J.S., Metayer, C., Gunier, R.B., Lubin, J., Crouse, V., Nishioka, M.G., Reynolds, P., Buffler, P.A., 2009. Residential exposure to polychlorinated biphenyls and organochlorine pesticides and risk of childhood leukemia. Environmental Health Perspectives 117, 1007–1013.

Wessels, D., Barr, D.B., Mendola, P., 2003. Use of biomarkers to indicate exposure of children to organophosphate pesticides: implications for a longitudinal study of children's environmental health. Environmental Health Perspectives 111, 1939–1946.

Xu, X., Dailey, A.B., Talbott, E.O., Ilacqua, V.A., Kearney, G., Asal, N.R., 2010. Associations of serum concentrations of organochlorine pesticides with breast cancer and prostate cancer in U.S. adults. Environmental Health Perspectives 118, 60–66.

Yanagisawa, R., Takano, H., Inoue, K., Koike, E., Sadakane, K., Ichinose, T., 2008. Effects of maternal exposure to di-(2-ethylhexyl) phthalate during fetal and/or neonatal periods on atopic dermatitis in male offspring. Environmental Health Perspectives 116, 1136–1141.

Zelikoff, J.T., Smialowicz, R., Bigazzi, P.E., Goyer, R.A., Lawrence, D.A., Maibach, H.I., Gardner, D., 1994. Immunomodulation by metals. Fundamental and Applied Toxicology 22, 1–7.

Journal of Immunotoxicology, 2012; Early Online: 1–10

ISSN 1547-691X print/ISSN 1547-6901 online
DOI: 10.3109/1547691X.2012.703252

informa
healthcare

RESEARCH ARTICLE

Immunotoxicity in mice induced by short-term exposure to methoxychlor, parathion, or piperonyl butoxide

Tomoki Fukuyama, Tadashi Kosaka, Koichi Hayashi, Lisa Miyashita, Yukari Tajima, Kunio Wada, Risako Nishino, Hideo Ueda, and Takanori Harada

Institute of Environmental Toxicology, Ibaraki, Japan

Abstract

Exposure to environmental agents can compromise numerous immunological functions. Immunotoxicology focuses on the evaluation of the potential adverse effects of xenobiotics on immune mechanisms that can lead to harmful changes in host responses such as: increased susceptibility to infectious diseases and tumorigenesis; the induction of hypersensitivity reactions; or an increased incidence of autoimmune disease. In order to assess the immunosuppressive response to short-term exposure to some commonly used pesticides, the studies here focused on the response of mice after exposures to the organochlorine pesticide methoxychlor, the organophosphorus pesticide parathion, or the agricultural insecticide synergist piperonyl butoxide. In these studies, 7-week-old mice were orally administered (by gavage) methoxychlor, parathion, or piperonyl butoxide daily for five consecutive days. On Day 2, all mice in each group were immunized with sheep red blood cells (SRBC), and their SRBC-specific IgM responses were subsequently assessed. In addition, levels of B-cells in the spleen of each mouse were also analyzed via surface antigen expression. The results of these studies indicated that treatments with these various pesticides induced marked decreases in the production of SRBC-specific IgM antibodies as well as in the expression of surface antigens in IgM- and germinal center-positive B-cells. Based on these outcomes, it is concluded that the short-term exposure protocol was able to detect potential immunosuppressive responses to methoxychlor, parathion, and piperonyl butoxide *in situ*, and, as a result, may be useful for detecting other environmental chemical-related immunotoxicities.

Keywords: Parathion, methoxychlor, piperonyl butoxide, Jurkat T-cell, apoptosis, T-dependent antigen response (TDAR)

Introduction

Exposure to environmental agents can compromise numerous immunological functions. In the United States alone, 20,000 pesticide products are on the market, and 1 billion pounds of active ingredients are applied annually for agricultural, industrial, and residential pest control (EPA, 2003). Against this background, studies in animals and humans have indicated that the immune system is a potential target, and that damage to this system can be associated with increased morbidity and even mortality. Immunotoxicologic analyses can evaluate the potential adverse effects of xenobiotics (e.g. chemicals, pesticides, drugs, biotechnology-derived products) on host immune mechanisms. Many of these effects can lead to harmful changes in host responses, including increased susceptibility to infectious diseases and tumorigenesis, the induction of hypersensitivity reactions, or an increased incidence of autoimmune disease (Herzyk and Holsapple, 2007).

Immunotoxicological testing has emerged in recent years as an important adjunct to routine safety evaluations of environmental chemicals and newly-developed pharmaceuticals, and has been incorporated into the guidelines issued by several regulatory authorities, including the Environmental Protection Agency (EPA, 1998), Food and Drug Administration (FDA, 2002), the European Medicines Agency (EMEA) (CPMP, 2000), and

Address for Correspondence: Dr Tomoki Fukyama, Laboratory of Immunotoxicology and Acute Toxicology, Toxicology Division, Institute of Environmental Toxicology, Uchimoriya-machi 4321, Joso-shi, Ibaraki 303-0043, Japan. Tel: 81297274628. Fax: 81297274518. E-mail: fukuyama@iet.or.jp

(Received 05 March 2012; revised 25 April 2012; accepted 12 June 2012)

the International Conference on Harmonization (ICH, 2006). The most recent immunotoxicology guidance documents recommend T-dependent antigen response (TDAR) tests, primarily because this assay represents a comprehensive evaluation of immune function based on an assessment of various components of the immune system (e.g., antigen-presenting cells, T-helper lymphocytes, and B-lymphocytes) involved in an antigen-specific antibody response (White et al., 2010).

Originally this test was configured as an IgM/complement dependent *ex vivo* plaque-forming cell (PFC) assay in mice, with sheep red blood cells (SRBC) as both the immunogen and the target for complement-mediated lysis. Subsequently, an enzyme-linked immunosorbent assay (ELISA)-based format was developed using SRBC as both the immunogen and antigen in the antibody detection system (Temple et al., 1993). SRBC-based TDAR assays (PFC and ELISA) have also been used in rats, and have ultimately gained acceptance as validated tests for detecting the immunosuppressant activity of drugs and chemicals (Ladics et al., 1998).

The above guidelines generally recommend using repeated doses, 28-day exposures, and adult animals to detect immunotoxicity caused by environmental chemicals. The use of long-term exposure offers the advantage of being able to compare results with those obtained from general toxicity tests. However, long-term exposure is time-consuming, costly, and may lead to immunotoxic drug resistance because the immune system is highly sensitive to the toxic effects of several types of chemicals (Fukuyama et al., 2011a); such a change would distort estimates of advanced immunotoxicity. Therefore, new short-term exposure protocols are needed to detect immunotoxicity. Previously, in the first stage of our studies, we developed a short-term method (administration via oral gavage for 3 days) for detecting thymocyte apoptosis induced by a typical immunosuppressant, methoxychlor (Fukuyama et al., 2010, 2011a). Indeed, methoxychlor induced prominent increases in several parameters indicative of induced thymocyte apoptosis, including Annexin V-FITC$^+$ cells, caspase (3/7, 8, and 9) activities, and DNA fragmentation. This type of dysregulation of apoptosis in the thymus is known to lead to various immune disorders, including immunodeficiency, tumorigenesis, allergies, and autoimmunity (Zhang et al., 2005). Our previous results demonstrated that short-term exposure has the potential to detect the immunosuppression caused by chemicals present in the environment.

In light of these previous results, the aim of this study was to develop a new short-term immunotoxicology protocol using several immunologic endpoints that tested short-term exposure to the organochlorine pesticide methoxychlor, the organophosphorus pesticide parathion, and the agricultural insecticide synergist piperonyl butoxide. These three chemicals were chosen on the basis of previous studies; parathion markedly inhibits antigen-specific-IgM production (Casale et al., 1984), and we previously showed that methoxychlor exposure results in atrophy of CD4$^+$CD8$^+$ T-lymphocytes in the thymus (Takeuchi et al., 2002, 2004; Fukuyama et al., 2011b). Piperonyl butoxide is an agricultural insecticide synergist used mainly with pyrethroids (Carson et al., 1988; Mitsumori et al., 1996; Emerson et al., 2001). Recent evidence suggests that piperonyl butoxide administration depletes T-lymphocytes in the spleen and thymus, induces hypoplasia of the bone marrow, and inhibits T-lymphocyte proliferation in lymphoid tissues (Mitsumori et al., 1996; Diel et al., 1999; Battaglia et al., 2010).

Materials and methods

Chemicals

Standard parathion ($C_{10}H_{14}NO_5PS$, 99.5% pure), standard methoxychlor ($C_{16}H_{15}Cl_3O_2$, > 97% pure), standard piperonyl butoxide ($C_{19}H_{30}O_5$, > 98% pure), dimethyl sulfoxide (DMSO), and acetone were purchased from Wako Pure Chemical Industries, Ltd. (Osaka, Japan). Corn oil was purchased from Hayashi Chemicals (Tokyo, Japan). For *in vitro* studies, parathion was dissolved in DMSO to 0.1% (w/v). Methoxychlor and piperonyl butoxide were dissolved in acetone to 0.1% (w/v).

Three concentrations (10, 100, and 1000 nmol/ml) of these pesticides were selected for use in the *in vitro* portions of these studies on the basis of results from preliminary cell viability analyses (data not shown); the exact concentrations chosen were based on the ability of each given agent to substantially inhibit cell viability but not cause 100% lethality.

For the *in vivo* portions of these studies, oral administration was used to introduce parathion, methoxychlor, and piperonyl butoxide (diluted in corn oil to a fixed final volume) into murine hosts. Based on the EPA Immunotoxicity Guidelines established in 1998, the highest dose level used in a host should 'not produce significant stress, malnutrition, or fatalities.' Accordingly, in this study, the maximum doses used were selected to be < 1/3 of the LD_{50} (dose at which ≥ 50% of animals would be expected to die) and concurrently to avoid the induction of clear systemic toxicity (i.e. changes in appearance, posture, behavior, respiration, consciousness, neurologic status, body temperature, excretion, etc.). The actual doses used are presented in Table 1.

Note, there is no overt relationship between the doses used in the *in vivo* and *in vitro* portions of these studies. The endpoints to be measured in each respective series of studies are distinct, and the information gleaned from the *in vitro* studies were only meant to be used for helping to explain outcomes (related to immunomodulation, etc.) that might appear in the agent-treated mice.

Animals

Female C3H/HeN (6-weeks-old) mice were purchased from Charles River Japan Laboratories (Atsugi, Kanagawa, Japan) and housed individually under controlled lighting

Table 1. Chemical doses used.

Chemical	Classification	Oral LD_{50} values (mg/kg)	Doses in this study (mg/kg)
Methoxychlor	organochlorine compound	2900[a]	0, 3, 30, 300
Parathion	organo-phosphorus compound	5[a]	0, 0.015, 0.15, 1.5
Piperonyl butoxide	agricultural insecticide synergist	2600[a]	0, 3, 30, 300

LD_{50}: dose at which 50% of animals died.
[a]Registry of Toxic Effects of Chemical Substances NIOSH CD-ROM (2003).

(lights on from 07:00 to 19:00 h), temperature (22 ± 3°C), humidity (55% ± 15%), and ventilation (at least 10 complete fresh-air changes hourly). Based on the EPA guideline (1998), mice are a model species recommended for use in immunotoxicity studies that test effects of agricultural chemicals (see as was done in Casale et al., 1984; Diel et al., 1999; Battaglia et al., 2010). Furthermore, for the immunotoxicity study, only one gender needed to be evaluated; in general, female animals are considered to yield more consistent outcomes than are male counterparts during evaluation of effects from test articles on host humoral immune responses. Therefore, in this study, female C3H/HeN were used. These particular hosts were also selected as our laboratory has historical immunotoxicity study data on this strain (data not shown). Food (Certified Pellet Diet MF, Oriental Yeast Co., Tokyo, Japan) and water were available *ad libitum*. This study was conducted in accordance with the Code of Ethics for Animal Experimentation of the Institute of Environmental Toxicology.

Cell culture

The human acute T-cell leukemia cell line Jurkat E6.1 was obtained from DS Pharma Biomedical Co., Ltd. (Tokyo, Japan). Jurkat E6.1 cells were cultured in 70-ml EasYFlasks (Nalge Nunc International K.K., Tokyo, Japan) in 5 ml of RPMI 1640 (Gibco, Tokyo, Japan) supplemented with 10% heat-inactivated fetal calf serum (FCS; Gibco) at 37°C in a 5% CO_2 atmosphere. The medium was changed three times per week.

Chemical treatment of the cells

The Jurkat E6.1 cells were seeded into flasks at 8×10^5 cells/ml. Quadruplicate flasks per dose per agent were then treated with 0, 10, 100, and 1000 nmol/ml of each test agent. Control cell cultures received vehicle-containing medium only. In all cases, the flasks were incubated for 30 min to 24 h at 37°C under 5% CO_2. At the end of the exposure time, the culture medium (containing all cells that were originally seeded, i.e. both live and dead) from each flask was transferred to a 5 ml tube and used in apoptosis assays. In general, to assess the extent of apoptosis, caspase-3/7, -8, and -9 activities as well as the proportions of AnnexinV-FITC$^+$ and caspase-3$^+$ cells were quantified.

Cell viability and caspase (3/7, 8, and 9) activity

Cell viability was determined in cultured cells by quantitation of ATP, an endpoint that is indicative of metabolically-active cells. Cell viability, caspase-3/7, -8, and -9 activities were measured at 30 min, 1, 2, 4, and 24 h after initiation of exposure to the chemicals by using a luciferin-luciferase system (CellTiter-Glo™ Luminescent Cell Viability Assay and Caspase-Glo™ assay, Promega, Tokyo, Japan). From each cell suspension, 3×10^4 cells were seeded in duplicate into opaque-walled 96-well plates (Corning Japan K.K., Tokyo, Japan). A microplate luminometer (Spectra MAX L, Molecular Devices, Osaka, Japan) was used to measure the caspase activities in relative light units (RLU).

Annexin-V and caspase-3 cell staining and flow cytometric analysis

Flow cytometric analysis of apoptotic cells was performed at 1 and 4 h after initiation of exposure by staining cells with fluorescein isothiocyanate (FITC)-conjugated Annexin-V, FITC-conjugated caspase-3, and propidium iodide. To assay the cells, an Annexin-V:FITC Apoptosis Detection Kit and an FITC Active Caspase-3 Apoptosis Kit (BD Pharmingen, San Diego, CA) was used, in accordance with manufacturer protocols. All samples were subsequently analyzed using a FACSCaliber flow cytometer (BD Pharmingen) and its accompanying Cell Quest program. For each sample, 10,000 events were collected and analyzed for antigen expression.

Chemical exposure of mice

After a 1-week acclimatization period, C3H/HeN mice (7-weeks-old) were allocated randomly to groups (n = 6 mice/group) for dosing, vehicle control, and no treatment (naïve group). Chemical dosages were as follows: methoxychlor, 3, 30, and 300 mg/kg/day; parathion, 0.015, 0.15, and 1.5 mg/kg/day: or piperonyl butoxide, 3, 30, and 300 mg/kg/day. On Days 1–5, mice were given an oral dose (by gavage, without anesthesia) of the test solution (methoxychlor, parathion, or piperonyl butoxide) or vehicle. On Day 2, a solution of sheep red blood cells (SRBC, 6×10^7 cells/animal; Nippon Bio-Supp. Center, Tokyo, Japan) was injected via the tail vein into all test and control mice for immunization.

One day after the last oral administration (i.e. on Day 6 of study), all mice were anesthetized and sacrificed by over-anesthesization with diethyl ether. Blood samples were taken from the inferior vena cava, and serum samples were assayed for SRBC-specific serum IgM. Each animal's spleen was removed and pooled in phosphate-buffered saline (PBS; Gibco). Single-cell suspensions of splenocytes in 5 ml of modified Eagle medium supplemented (MEM; Gibco) containing 5% heat-inactivated FCS were prepared by passage through a stainless-steel screen and sterile 70-μm nylon cell strainers (Falcon, Tokyo, Japan). The number of lymphocytes in the spleen preparation was then determined using a Coulter counter Z2 (Beckman Coulter, Tokyo, Japan).

SRBC-specific IgM responses in serum

Levels of SRBC-specific serum IgM were determined using a modified version of the method of Temple et al. (1993). In brief, SRBC-membrane antigen was extracted with Tris-HCL and 0.1% SDS in PBS. The samples were then extensively dialyzed for 2 days against PBS. The protein content of each conjugated sample was determined by the method of Lowry et al. (1951). Specific serum IgM was then measured by means of an ELISA using flat-bottomed microplates (Nalge Nunc) whose wells had been coated with SRBC-membrane antigen (2 μg/ml in coating buffer; BD Pharmingen) during an overnight incubation at 4°C. Following washing of each well five times with wash buffer (BD Pharmingen), and blocking of potential non-specific binding by incubation with assay diluent (BD Pharmingen) for 2 h at room temperature (RT), dilutions of each mouse serum sample (in assay diluent, from 1:4 to 1:16,384) was added to each well and the plates incubated for 2 h at RT. After gentle rinsing with wash buffer to remove all unbound materials, peroxidase conjugated anti-mouse IgM (secondary antibody; Rochland Inc. PA, dilution 1:15,000) was added to each well and the plate incubated for 2 h at RT. The wells were then rinsed again to remove non-adherent anti-mouse IgM. Finally, to quantify the amount of bound antibodies in each well, tetramethylbenzidine (TMB; 100 μl/well) substrate was added to each well and the plate incubated in the dark at RT for 30 min. Optical density measurements were then made at 450 nm in a Spectra MAX 190 microplate reader (Molecular Devices, Osaka, Japan).

IgM plaque-forming cell response to SRBC in splenocytes

The IgM plaque-forming cell (PFC) response to SRBC was determined by using a modified version of the methods of Cunningham (1965) and Jerne and Nordin (1963). Briefly, 1×10^6 cells were incubated with 1% SRBC and a 1:30 dilution of guinea pig complement (Denka Seiken Co., Tokyo) for 10 min at 4°C. The cells were applied to a Cunning-ham chamber (Takahashi Giken Glass Co., Ltd, Tokyo, Japan), and incubated for 1.5 h at 37°C in a 5% CO_2 atmosphere. The number of plaques in each sample was then counted using a stereo-microscope.

Flow cytometric analysis

Isolated splenocytes were stained with fluorescein isothiocyanate (FITC)-conjugated peanut agglutinin (Vector Laboratories, Inc., Burlingame, CA), FITC-conjugated rat anti-mouse IgM (R6-60.2; BD), phycoerythrin (PE)-conjugated rat anti-mouse IgD (clone 11-26c.2a; BD), PE-cyano dye (Cy)5-conjugated rat anti-mouse CD45R/B220 (clone RA3-6B2; BD), and/or peridinin chlorphyll protein (PerCP)-Cy5.5-conjugated rat anti-mouse CD19 (clone 1D3; BD) to perform the flow analyses. To avoid non-specific binding, 1×10^6 cells were incubated with 20% normal goat serum (Sigma, St. Louis, MO) for 10 min at 4°C; this was followed by incubation with FITC-, PE-, PE-Cy5-, and PerCP-Cy5.5-conjugated monoclonal antibodies for 30 min at 4°C in the dark. The cells were washed twice with FCS-MEM, re-suspended at 1×10^6 cells per tube in 1 ml of PBS, and then analyzed with the FACSCaliber flow cytometer and its Cell Quest program. For each sample, 10,000 events were collected and analyzed for antigen expression.

Statistical analysis

The data were transformed logarithmically to equalize the variance, and analysis of variance (ANOVA) was used to evaluate the results. For statistically significant ANOVA, the differences between groups were assessed by using Dunnett's multiple comparison test. A p-value < 0.05 was considered to indicate statistical significance.

Results

Preliminary in vitro study (confirmation of apoptosis)

In vitro analyses were performed to evaluate the extent of apoptosis resulting from parathion, methoxychlor, or piperonyl butoxide treatment. Caspase-3/7 activities (Figures 1a,d, and g) increased significantly relative to control levels in the methoxychlor (1–24 h: 1000 nmol), parathion (2–24 h: 1000 nmol), and piperonyl butoxide (0.5–24 h: 1000 nmol) treatment groups. Caspase-8 activity (Figures 1b, e, and h) increased significantly relative to control values in the methoxychlor (4 h: 1000 nmol) and piperonyl butoxide (2–4 h: 1000 nmol) treatment groups. Caspase-9 activity (Figures 1c, f, and i) increased significantly relative to control levels in the methoxychlor (2–4 h: 1000 nmol, 24 h: 100 and 1000 nmol) and piperonyl butoxide (2–24 h: 1000 nmol) treatment groups.

Flow cytometric analysis was used to evaluate the extent of apoptosis resulting from methoxychlor, parathion, or piperonyl butoxide treatment. The analyses revealed that the proportion of Annexin-V^+PI^- cells (Figure 2) increased significantly relative to the same values for the controls in the methoxychlor (1 h: 1000 nmol, 4 h: 100 and 1000 nmol), parathion (1 and 4 h: 1000 nmol), and piperonyl butoxide (1 and 4 h: 1000 nmol) treatment groups. The proportion of caspase-3^+ cells (Figure 3) increased significantly relative to those seen in the controls as a result of the methoxychlor (1 h: 1000 nmol, 4 h: 100 and 1000 nmol), parathion (4 h: 100 and 1000 nmol), and piperonyl butoxide (4 h: 1000 nmol) treatments.

In vivo study (confirmation of anti-SRBC IgM responses in mice)

The SRBC-specific IgM responses in serum are shown in Figure 4a The 30 and 300 mg methoxychlor/kg, as well as the 1.5 mg parathion/kg, treatments caused a significant decrease in responses relative to those seen with the vehicle controls. The piperonyl butoxide treatments cause a decreasing trend, but this was mild; no significant differences from control were noted.

The IgM plaque-forming cell (PFC) responses to SRBC in splenocyte are shown in Figure 4b. The 300 mg methoxychlor/kg treatment caused a significant decrease

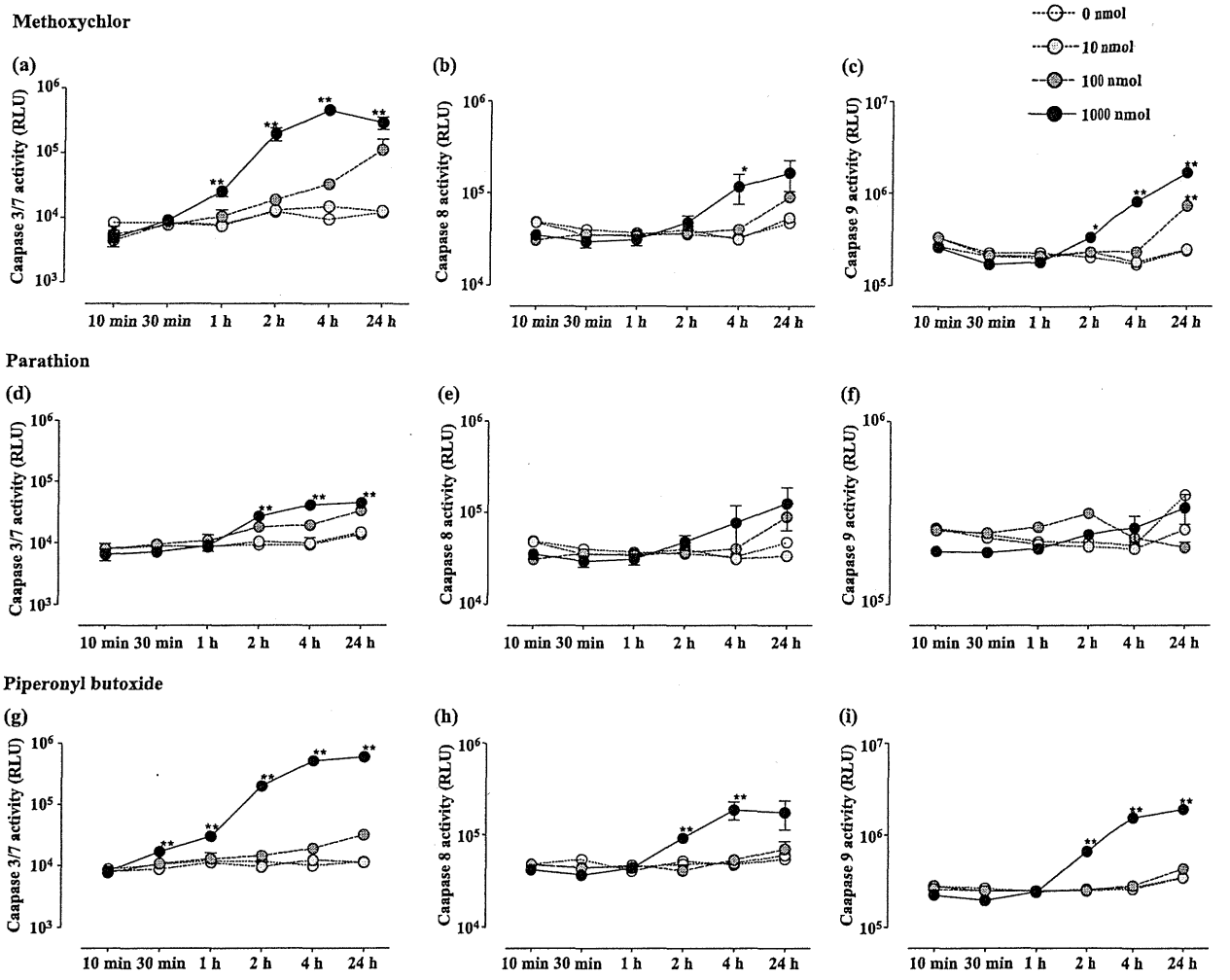

Figure 1. Caspase-3/7, -8, and -9 activities in Jurkat T-cells treated with test chemicals for 10 min to 24 h. Caspase-3/7 (a: Methoxychlor; d: Parathion; g: Piperonyl butoxide), Caspase-8 (b: Methoxychlor; e: Parathion; h: Piperonyl butoxide), and Caspase-9 (c: Methoxychlor; f: Parathion; i: Piperonyl butoxide). All activities are expressed as mean (RLU) ± SD. Value significantly differs from control at * $p < 0.05$ and ** $p < 0.01$.

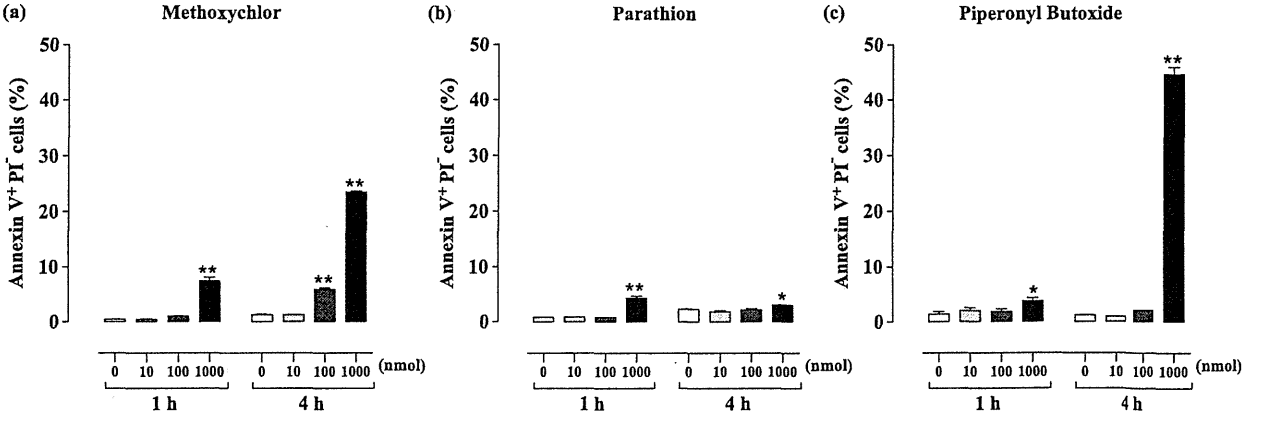

Figure 2. Annexin V-FITC positive cells among Jurkat T-cells treated with test chemicals for 1 or 4 h. (a) Methoxychlor; (b) Parathion; and (c) Piperonyl butoxide. Annexin V+-FITC+ cells are expressed as the mean (proportion of total, %) ± SD. Value significantly differs from control at * $p < 0.05$ and ** $p < 0.01$.

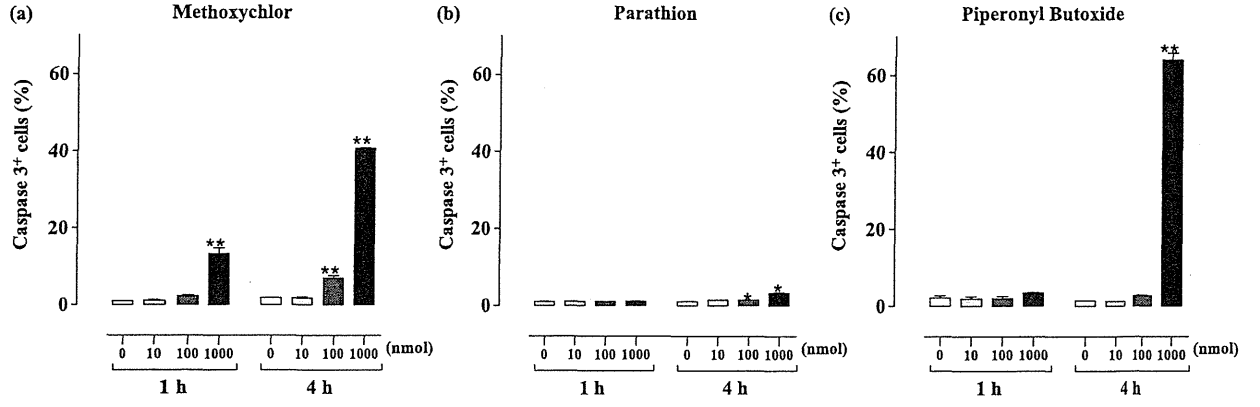

Figure 3. Caspase-3+ cells among Jurkat T-cells treated with test chemicals for 1 or 4 h. (a) Methoxychlor; (b) Parathion; and (c) Piperonyl butoxide. Caspase-3+ cells are expressed as the mean (proportion of total, %) ± SD. Value significantly differs from control at * $p < 0.05$ and ** $p < 0.01$.

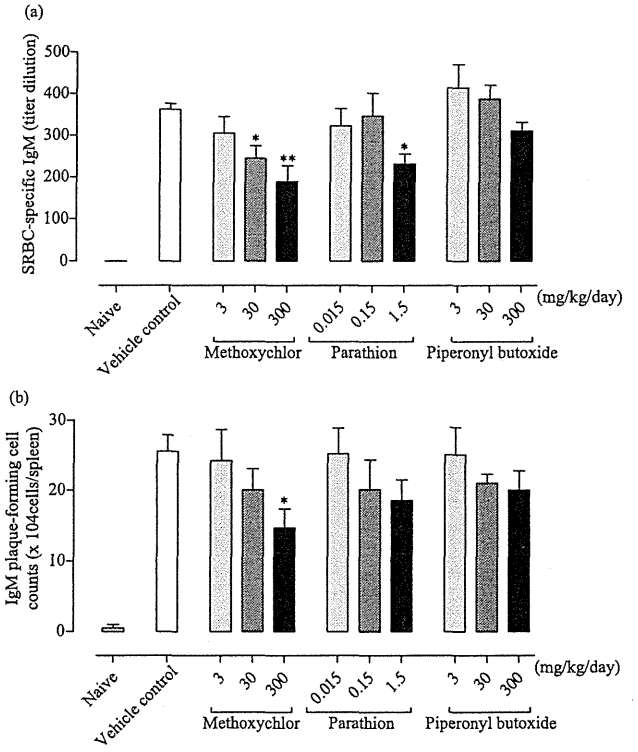

Figure 4. Anti-SRBC IgM response in C3H/He female mice treated with test chemicals. (a) SRBC-specific IgM response in serum. (b) Splenocyte IgM plaque-forming cell responses to SRBC. Values (titer dilution and cell counts) are expressed as mean ± SD. Value significantly differs from control at * $p < 0.05$ and ** $p < 0.01$.

in this parameter relative to the value seen with the vehicle controls. Both the parathion and piperonyl butoxide treatments led to a decreasing trend in this measure, but these decreases were mild and the final values did not significantly differ from the control values.

In vivo study (flow cytometric analysis)

To evaluate the activation of B-lymphocytes in the spleen following methoxychlor, parathion, and piperonyl butoxide treatment, flow cytometric analysis was performed using the lymphocytes stained with anti-CD19, -CD45R/B220, -IgD, -IgM, and -peanut agglutinin antibodies. Total cell counts in the spleen are shown in Figure 5a. The piperonyl butoxide 300 mg/kg treatment caused a significant decrease in this value relative to that in the vehicle controls. The methoxychlor treatments led to a decreasing trend as well, but no significant differences were noted. The numbers and ratio of IgM-positive B-lymphocytes ($B220^+IgD^+IgM^+$) are shown in Figures 5d and e. The 300 mg methoxychlor/kg, 1.5 mg parathion/kg, and the 30 and 300 mg piperonyl butoxide/kg treatments led to a significant decrease relative to values seen in the corresponding

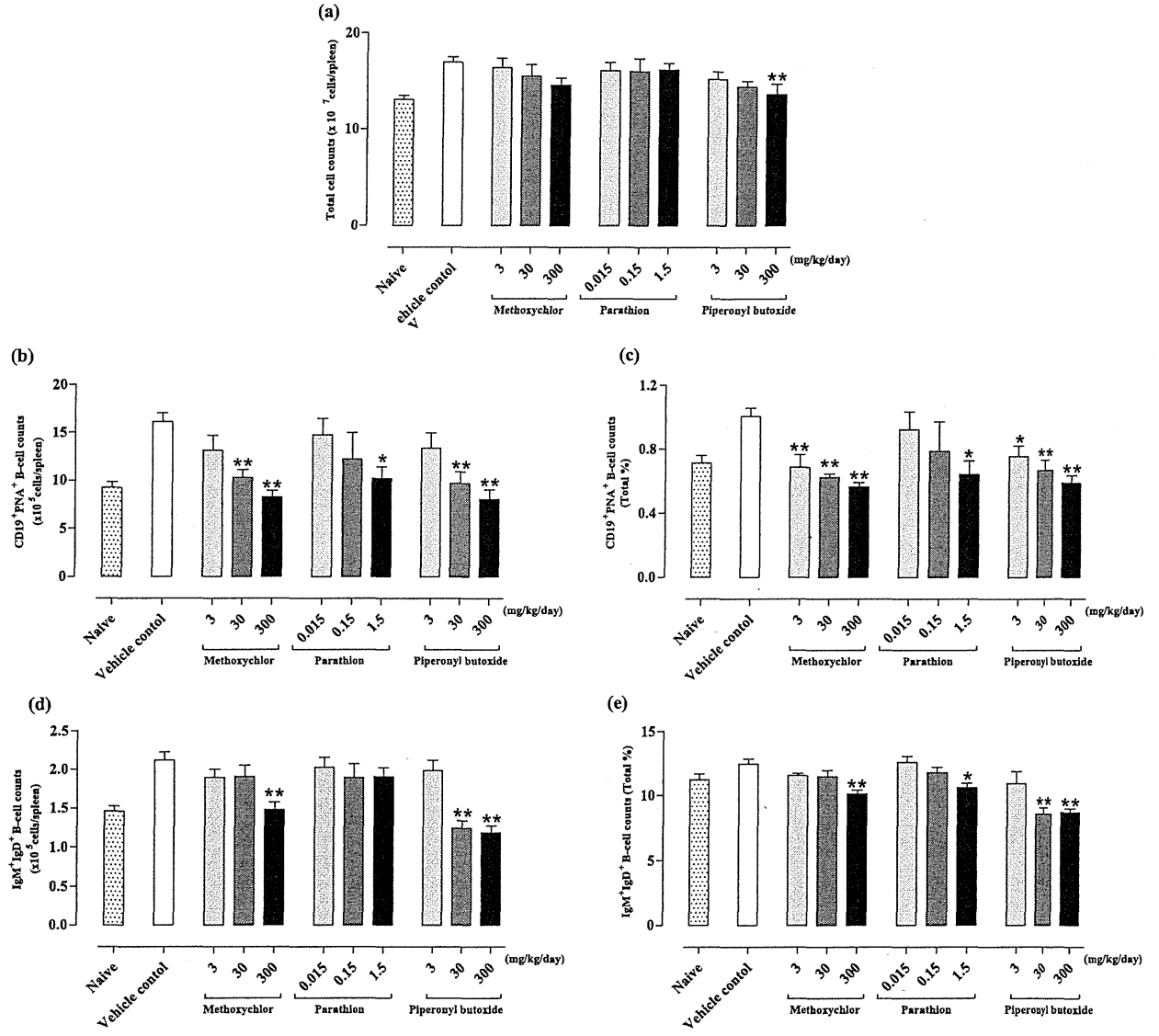

Figure 5. Flow cytometric analyses of splenocytes from C3H/He female mice treated with test chemicals. (a) Total cell counts; (b) germinal center-positive B-lymphocyte counts (CD19+PNA+); (c) germinal center-positive B-lymphocyte counts (CD19+PNA+, proportion of total, %); (d) IgM+ B-lymphocyte counts (B220+IgD+IgM+); and (e) IgM+ B-lymphocyte counts (B220+IgD+IgM+, proportion of total, %) in spleen. Counts are expressed as mean ± SD. Value significantly differs from control at * $p < 0.05$ and ** $p < 0.01$.

cells from vehicle control hosts. The numbers and ratio of germinal center B-lymphocytes ($CD19^+PNA^+$) are shown in Figures 5b and c. The treatments with 3, 30, and 300 mg methoxychlor/kg, 1.5 mg parathion/kg, and 3, 30, and 300 mg piperonyl butoxide/kg caused significant decreases in this parameter relative to the values noted with the vehicle controls.

Discussion

Our primary objective in this study was to improve upon the current method of detecting environmental chemical-related immunotoxicity. To that end, we exposed mice by using a short-term exposure protocol (i.e. 5 days) to commonly used immunosuppressive chemicals, namely the organochlorine agent methoxychlor, the organophosphorus agent parathion, and the agricultural insecticide synergist piperonyl butoxide. We then assessed the effects of this short-term exposure via several types of detection methods, including induction of lymphocyte apoptosis in Jurkat T-cells, anti-SRBC IgM responses in serum and spleen, and numbers of IgM- and germinal center-positive B-lymphocytes in the spleen. Our results showed that methoxychlor, parathion, and piperonyl butoxide each could modulate the apoptosis of Jurkat T-cells *in vitro*. To assess apoptosis, caspase activities (3/7, 8, and 9), and the proportion of Annexin V- and caspase-3^+ cells were examined. In mice, chemical-related immunotoxicity was detected by using our short-term exposure protocol. Indeed, all three chemicals induced

prominent immuno-suppressive responses, including reducing the anti-SRBC IgM response (SRBC-specific IgM levels in serum and the IgM PFC response to SRBC in splenocyte), and the numbers of IgM- and germinal center-positive B-lymphocytes in the spleen.

Apoptosis is an essential process underlying multicellular organism development and function. In the immune system, apoptosis is required for lymphocyte development and homeostasis. Dysregulation of apoptosis leads to a variety of immune disorders, including immunodeficiency, tumorogenesis, allergies, and autoimmunity (Zhang et al., 2005). Detection of chemical-induced thymocyte apoptosis *in vivo* is difficult, however, because of the rapid clearance of apoptotic cells by phagocytes (Savill and Haslett, 1995; Kamath et al., 1997; Pryputniewicz et al., 1998). Therefore, in the current study, we first confirmed the immunosuppressive effects of methoxychlor, parathion, and piperonyl butoxide by assessing changes in the occurrence of apoptosis in a human leukemia cell line, Jurkat E6.1.

We observed a significant increase in caspase activities (3/7, 8, and 9) and in the proportion of Annexin V^+ and caspase-3^+ cells that resulted from exposure to the test chemicals (Figures 1–3). Annexin V^+ staining is reported to detect apoptosis at an early stage, allowing visualization of alterations in the cell membrane that occur when phosphatidylserine residues move to the external leaflet of the plasma membrane (Morris et al., 1984; Vermes et al., 1995). Caspases are required in the apoptotic pathway; therefore, measurement of caspases-3/7, -8, and -9 reliably indicates caspase-dependent apoptosis (Gurtu et al., 1997). Caspase-3 and -7 were the first caspases linked to apoptosis, and, together with caspase-8 and -9, act upstream of DNA fragmentation in the pathway. Our findings suggest that methoxychlor and piperonyl butoxide induced T-lymphocyte apoptosis *in vitro* via several caspase pathways. In contrast, parathion induced T-lymphocyte apoptosis via mainly the caspase-3 pathway. The immunomodulation demonstrated *in vitro* in this study may reflect what could occur *in situ*, i.e. these types of reactions in a growing fetus might predispose the highly sensitive fetal immune system to a loss of tolerance to self-antigens and lead to a subsequent increased risk for autoimmune disease and allergies as the offspring develops after birth.

On the basis of our preliminary *in vitro* data, we then performed our primary study using female C3H/He mice (7-weeks-old). To detect environmental chemical-related immunotoxicity, we focused on short-term exposure (i.e., 5 days) and several immune endpoints. Among them, we used a T-dependent antigen response (TDAR) test primarily and measured the antigen (SRBC)-specific IgM response using an ELISA and a PFC assay. There is no doubt that the antigen-specific IgM antibody plays a key role in all types of immune response to immunotoxic chemicals (Anderson et al., 2006). The SRBC-specific IgM ELISA utilizes solubilized, hemoglobin-free SRBC membranes, and measures SRBC-specific antibodies in serum that are generated by all antibody-producing tissues (i.e. spleen, lymph nodes, bone marrow), reflecting the systemic humoral immune response (Temple et al., 1993). On the other hand, the PFC assay has been well characterized across multiple labs, and is likely the most validated endpoint in immunotoxicology.

Combining the use of these two assays allows for studies to evaluate mechanisms of action of xenobiotic-induced immunotoxicity (Herzyk and Holsapple, 2007). In our study, methoxychlor, parathion, and piperonyl butoxide induced a prominent decrease both in antigen-specific serum IgM levels and IgM PFC counts compared to the vehicle controls. Generally speaking, these chemicals have immunosuppressive effects, and our preliminary study suggests that apoptosis was induced in Jurkat T-cells. Therefore, this down-regulation demonstrates that our protocol and methods were effective for identifying environmental chemical-related immunotoxicity.

In addition to the serum and spleen antigen-specific IgM responses, we analyzed the IgM- and IgD-expressing B-cell populations in spleen by use of flow cytometry. The first antibodies to be produced in a humoral immune response are always IgM, because IgM can be expressed without isotype switching. Surface IgM- and IgD-expressing B-cells are necessary for IgM production (Janeway et al., 2004). According to our results, significant decreases in the IgM-expressing B-lymphocyte population were observed in both the methoxychlor- and piperonyl butoxide-treated groups (Figure 5). This down-regulation of IgM-expressing B-lymphocytes would thus be a useful endpoint for identifying chemical-related immunotoxicity.

Some B-cells are activated at the T-/B-lymphocyte border and migrate to form a germinal center within a primary follicle. Germinal centers are sites of rapid B-lymphocyte proliferation and differentiation (Janeway et al., 2004). Therefore, the germinal center and germinal center B-lymphocyte development represent major responses to exposure to T-lymphocyte-dependent antigen (Vieira and Rajewsky, 1990; Takahashi et al., 1998). We used PNA as a representative germinal center B-lymphocyte surface antigen because all germinal center B-lymphocytes bind PNA, beginning at the earliest stages of germinal center formation (Shinall et al., 2000). We observed dose-dependent and significant decreases in the PNA^+ B-lymphocyte population in each chemical-treated group (Figure 5). These results support our belief that this short-term exposure protocol could be used to detect immune suppression followed by chemical treatment.

Conclusions

Our protocol detected environmental chemical (i.e. methoxychlor, parathion, and piperonyl butoxide)-induced immunotoxic responses, such as increased apoptosis in lymphocytes *in vitro*, decreased antigen-specific

IgM responses, and decreased IgM- and germinal center-positive B-lymphocyte counts. Additional studies to confirm these results should be expanded to include other parallel changes in cellular function that can occur in response to chemical exposure, as well as immunologic or histologic markers. Our ongoing studies continue to focus on the detection of weak immunotoxic reactions using this short-term exposure protocol. However, our results and protocols have yet to be formally validated, which is a pre-requisite for inclusion in guidelines endorsed by regulatory authorities. Validation experiments therefore represent the next important task for us to undertake.

Acknowledgments

The authors wish to thank Dr Y. Shutoh, Dr H. Fujie, Dr A. Motomura, and Dr Y. Komatsu of the Institute of Environmental Toxicology (Ibaraki, Japan) for their technical assistance. This work was supported by a research Grant-in-Aid from the Ministry of Health, Labor and Welfare of Japan.

Declaration of interest

The authors report no conflicts of interest. The authors alone are responsible for the content and writing of the paper.

References

Anderson, S. E., Munson, A. E., and Meade, B. J. 2006. Analysis of immunotoxicity by enumeration of antibody-producing B cells. In: *Current Protocols in Toxicology*. Unit 18.11. (Bus, J. S., Costa, L. G., Hodgson, E., Lawrence, D. A., and Reed, D., Eds.). Hoboken, NJ: John Wiley and Sons, pp. 1–18.

Battaglia, C. L., Gogal, R. M. Jr., Zimmerman, K., and Misra, H. P. 2010. Malathion, lindane, and piperonyl butoxide, individually or in combined mixtures, induce immunotoxicity via apoptosis in murine splenocytes *in vitro*. *Int. J. Toxicol.* 29:209–220.

Carson, D. S., Tribble, P. W., and Weart, C. W. 1988. Pyrethrins combined with piperonyl butoxide (RID) vs. 1% permethrin (NIX) in the treatment of head lice. *Am. J. Dis. Child.* 142:768–769.

Casale, G. P., Cohen, S. D., and DiCapua, R. A. 1984. Parathion-induced suppression of humoral immunity in inbred mice. *Toxicol. Lett.* 23:239–247.

Committee on Proprietary Medicinal Products. 2000. *Note for Guidance on Repeat-Dose Toxicity*, CPMP/SWP/1042/99. Available online at: http://www.emea.eu.int.

Cunningham, A. J. 1965. A method of increased sensitivity for detecting single antibody-forming cells. *Nature* 207:1106–1107.

Diel, F., Horr, B., Borck, H., Savtchenko, H., Mitsche, T., and Diel, E. 1999. Pyrethroids and piperonyl-butoxide affect human T-lymphocytes in vitro. *Toxicol. Lett.* 107:65–74.

Emerson, M. R., Biswas, S., and LeVine, S. M. 2001. Cuprizone and piperonyl butoxide, proposed inhibitors of T-cell function, attenuate experimental allergic encephalomyelitis in SJL mice. *J. Neuroimmunol.* 119:205–213.

EPA. 1998. United States Environmental Protection Agency. *Health Effects Test Guidelines: Immunotoxicity*. 1998, OPPTS 870.7800. Available online at: http://www.epa.gov/opptsfrs/publications.

EPA. 2003. United States Environmental Protection Agency. Office of Research and Development. Human Health Research Strategy (PUB EPA/600/R-02/050). Washington, DC: US EPA, 2003.

FDA. 2002. United States Food and Drug Administration. *Guidance for Industry: Immunotoxicology Evaluation of Investigational New Drugs*. Available online at: http://www.fda.gov/cder/guidance.

Fukuyama, T., Kosaka, T., Tajima, Y., Hayashi, K., Shutoh, Y., and Harada, T. 2011a. Detection of thymocytes apoptosis in mice induced by organochlorine pesticides methoxychlor. *Immunopharmacol. Immunotoxicol.* 33:193–200.

Fukuyama, T., Tajima, Y., Ueda, H., Hayashi, K., and Kosaka, T. 2011b. Prior exposure to immunosuppressive organophosphorus or organochlorine compounds aggravates the T_H1- and T_H2-type allergy caused by topical sensitization to 2,4-dinitrochlorobenzene and trimel-litic anhydride. *J. Immunotoxicol.* 8:170–182.

Fukuyama, T., Tajima, Y., Ueda, H., Hayashi, K., Shutoh, Y., Harada, T., and Kosaka, T. 2010. Apoptosis in immunocytes induced by several types of pesticides. *J. Immunotoxicol.* 7:39–56.

Gurtu, V., Kain, S. R., and Zhang, G. 1997. Fluorometric and colorimetric detection of caspase activity associated with apoptosis. *Anal. Biochem.* 251:98–102.

Herzyk, D. J., and Holsapple, M. 2007. Immunotoxicity evaluation by immune function tests: Focus on the T-dependent antibody response (TDAR). *J. Immunotoxicol.* 4:143–147.

ICH. 2006. International Conference on harmonization of technical requirements for registration of pharmaceuticals for human use. *ICH Harmonised Tripartite Guideline Immunotoxicity Studies For Human Pharmaceuticals S8*. Switzerland. ICH.

Janeway, C. A., Travers, P., Walport, M., and Shlomchik, M. J. (Eds.) 2004. *Immunobiology*, 6th Edition. New York: Garland Science.

Jerne, N. K., and Nordin, A. A. 1963. Plaque formation in agar by single antibody-producing cells. *Science* 140:405.

Kamath, A. B., Xu, H., Nagarkatti, P. S., and Nagarkatti, M. 1997. Evidence for the induction of apoptosis in thymocytes by 2,3,7,8-tetrachlorodibenzo-p-dioxin *in vivo*. *Toxicol. Appl. Pharmacol.* 142:367–377.

Ladics, G. S., Smith, C., Elliott, G. S., Slone, T. W., and Loveless, S. E. 1998. Further evaluation of incorporation of an immunotoxicological functional assay for assessing humoral immunity for hazard identification purposes in rats in a standard toxicology study. *Toxicology* 126:137–152.

Lowry, O. H., Rosebrough, N. J., Farr, A. L., and Randall, R. J. 1951. Protein measurement with the Folin phenol reagent. *J. Biol. Chem.* 193:265–275.

Mitsumori, K., Takegawa, K., Shimo, T., Onodera, H., Yasuhara, K., and Takahashi, M. 1996. Morphometric and immunohistochemical studies on atrophic changes in lymphohematopoietic organs of rats treated with piperonyl butoxide or subjected to dietary restriction. *Arch. Toxicol.* 70:809–814.

Morris, R. G., Hargreaves, A. D., Duvall, E., and Wyllie, A. H. 1984. Hormone-induced cell death. 2. Surface changes in thymocytes undergoing apoptosis. *Am. J. Pathol.* 115:426–436.

Pryputniewicz, S. J., Nagarkatti, M., and Nagarkatti, P. S. 1998. Differential induction of apoptosis in activated and resting T-cells by 2,3,7,8-tetrachlorodibenzo-p-dioxin (TCDD) and its repercussion on T-cell responsiveness. *Toxicology* 129:211–226.

Registry of Toxic Effects of Chemical Substances NIOSH CD-ROM (2003).

Savill, J., and Haslett, C. 1995. Granulocyte clearance by apoptosis in the resolution of inflamemation. *Semin. Cell Biol.* 6:385–933.

Shinall, S. M., Gonzalez-Fernandez, M., Noelle, R. J., and Waldschmidt, T. J. 2000. Identification of murine germinal center B-cell subsets defined by the expression of surface isotypes and differentiation antigens. *J. Immunol.* 164:5729–5738.

Takahashi, Y., Dutta, P. R., Cerasoli, D. M., and Kelsoe, G. 1998. In situ studies of the primary immune response to (4-hydroxy-3-nitrophenyl)acetyl. V. Affinity maturation develops in two stages of clonal selection. *J. Exp. Med.* 187:885–895.

Takeuchi, Y., Kosaka, T., Hayashi, K., Ishimine, S., Ohtsuka, R., Kuwahara, M., Yoshida, T., Takahashi, N., Takeda, M., Maita, K., and Harada, T. 2004. Alterations in the developing immune system of the rat after perinatal exposure to methoxychlor. *J. Toxicol. Pathol.* 17:165–170.

Takeuchi, Y., Kosaka, T., Hayashi, K., Takeda, M., Yoshida, T., Fujisawa, H., Teramoto, S., Maita, K., and Harada, T. 2002. Thymic atrophy induced by methoxychlor in rat pups. *Toxicol. Lett.* 135:199–207.

Temple, L., Kawabata, T. T., Munson, A. E., and White, K. L. Jr. 1993. Comparison of ELISA and plaque-forming cell assays for measuring the humoral immune response to SRBC in rats and mice treated with benzo[a]pyrene or cyclophosphamide. *Fundam. Appl. Toxicol.* 21:412–419.

Vermes, I., Haanen, C., Steffens-Nakken, H., and Reutelingsperger, C. 1995. A novel assay for apoptosis. Flow cytometric detection of phosphatidylserine expression on early apoptotic cells using fluorescein-labeled Annexin V. *J. Immunol. Meth.* 184:39–51.

Vieira, P., and Rajewsky, K. 1990. Persistence of memory B-cells in mice deprived of T cell help. *Int. Immunol.* 2:487–494.

White, K. L., Musgrove, D. L., and Brown, R. D. 2010. The sheep erythrocyte T-dependent antibody response (TDAR). *Methods Mol. Biol.* 598:173–184.

Zhang, N., Hartig, H., Dzhagalov, I., Draper, D., and He, Y. W. 2005. The role of apoptosis in the development and function of T-lymphocytes. *Cell Res.* 15:749–769.

Establishment of a Stable Human Cell Line, HPL-A3, for Use in Reporter Gene Assays of Cytochrome P450 3A Inducers

Masashi Sekimoto, Shinsuke Sano,† Takuomi Hosaka,‡ Kiyomitsu Nemoto, and Masakuni Degawa*

Department of Molecular Toxicology and Global Center of Excellence Program, School of Pharmaceutical Sciences, University of Shizuoka; 52–1 Yada, Suruga-ku, Shizuoka 422–8526, Japan.
Received November 4, 2011; accepted February 22, 2012; published online March 5, 2012

We have established a stable human cell line, termed HPL-A3, by co-transfection of a human pregnane X receptor (hPXR) expression vector and a reporter plasmid (p3A4-hPXRE-Luc) containing a luciferase gene and a promoter/enhancer region of the human *cytochrome P450 3A4* (*CYP3A4*) gene into a human hepatoma-derived cell line, HepG2. We then examined the usefulness of HPL-A3 for a chemically activated luciferase expression (CALUX) assay of human CYP3A inducers. The induction of CALUX in HPL-A3 by hPXR activators, including rifampicin, occurred in time- and concentration-dependent fashions, whereas no such induction was observed using rat/mouse PXR activators, such as pregnenolone-16α-carbonitrile and dexamethasone. The hPXR activator-mediated induction of CYP3As, especially CYP3A4, was observed at levels of both mRNA and enzyme activity. Furthermore, there were positive correlations between chemical-mediated inductions of CALUX and CYP3A4 mRNA levels. In addition, the induction of CALUX by dihydropyridine calcium channel blockers, which are known to act as CYP3A inducers in rats, was observed in HPL-A3 cells. Interestingly, expression levels of not only hPXR but also of vitamin D receptor (VDR), a transcription factor that positively regulates CYP3A subfamily genes, were significantly increased in HPL-A3 cells compared with those in the parental cell line, HepG2. Consequently, VDR ligand (1,25-dihydroxyvitamin D_3)-mediated inductions of CALUX and CYP3A4 mRNA were observed in the cells. These findings verified the usefulness of HPL-A3 for the screening of CYP3A inducers, which can activate the hPXR and/or hVDR.

Key words cytochrome P450 3A4; pregnane X receptor; vitamin D receptor; chemically activated luciferase expression; calcium channel blocker

Human cytochrome P450 3A (CYP3A) subfamily enzymes, especially CYP3A4, play important roles in the metabolism of xenobiotics, including drugs, agricultural chemicals and endocrine disrupters.[1,2] Accordingly, studies on xenobiotic-mediated induction/inhibition of CYP3A enzymes are important for understanding the therapeutic/toxic effects of xenobiotics, including drugs. We can now assess the inhibitory effects of xenobiotics on the activity of human CYP3A enzymes by *in vitro* assays using commercially available human hepatic microsomes and/or enzymes.[3] However, only a few *in vitro* induction assays are established, because there are only a limited number of cell lines capable of xenobiotic-mediated induction of CYP3A enzymes.[4] The lack of such responsiveness of cultured cell lines to xenobiotics is caused by a considerable decrease in the expression level of pregnane X receptor (PXR),[5] a main transcription factor for the *CYP3A* subfamily genes.[6,7] Likewise, vitamin D receptor (VDR)[8] and constitutive androstane receptor (CAR),[9] which also act as a transcriptional activators of *CYP3A* subfamily genes, are expressed at low levels or not at all in human hepatoma-derived cell lines, including HepG2.[5,10]

Recently, several stable cell lines for a human PXR (hPXR)-based reporter gene assay for the screening of CYP3A4 inducers have been established by co-transfection into human cell lines of an hPXR expression vector and a plasmid containing a reporter gene and hPXR-binding elements.[11–15] However, the available data on the xenobiotic-mediated induction of CYP3A enzymes at the levels of mRNA and activity in the reported cell lines are limited.

In the present study, to further develop an improved tool for the assessment of human CYP3A inducers, we have established a human cell line applicable for not only the reporter gene assay but also for assays of mRNA levels and enzyme activities. We confirmed the usefulness of the established cell line, termed HPL-A3, in assays of human CYP3A inducers.

MATERIALS AND METHODS

Chemicals Rifampicin (RIF), clotrimazole (CLO), pregnenolone-16α-carbonitrile (PCN), dexamethasone (DEX), tamoxifen citrate (TAM), nimodipine (NIM) and 1,25-dihydroxyvitamine D_3 (VD_3) were purchased from Sigma Chemical Co. (St. Louis, MO, U.S.A.). Nicardipine hydrochloride (NIC), nifedipine (NIF), nisoldipine (NIS), nitrendipine (NIT), and dimethylsulfoxide (DMSO) were obtained from Wako Pure Chemical (Osaka, Japan). The structures of chemicals used in this study are shown in Fig. 1. All the chemicals examined were dissolved in DMSO.

Construction of Reporter Plasmid The nuclear hormone receptor binding motif (ER6, −172 to −149) and distal nuclear receptor (dNR)-binding elements, such as dNR-1 (−7733 to −7719) and dNR-2 (−7489 to −7472), in a promoter/enhancer region of the human *CYP3A4* gene play a crucial role in the PXR-mediated induction of the gene.[16] Therefore, an hPXR reporter plasmid, termed p3A4-hPXRE-Luc, containing a

†Present address: *Department of Hospital Pharmacy, Hamamatsu University School of Medicine; 1–20–1 Handayama, Higashi-ku, Hamamatsu, Shizuoka 431–3192, Japan.*

‡Present address: *Department of Toxicology, Faculty of Pharmaceutical Sciences, Setsunan University; 45–1 Nagaotouge-cho, Hirakata, Osaka 573–0101, Japan.*

* To whom correspondence should be addressed. e-mail: degawa@u-shizuoka-ken.ac.jp

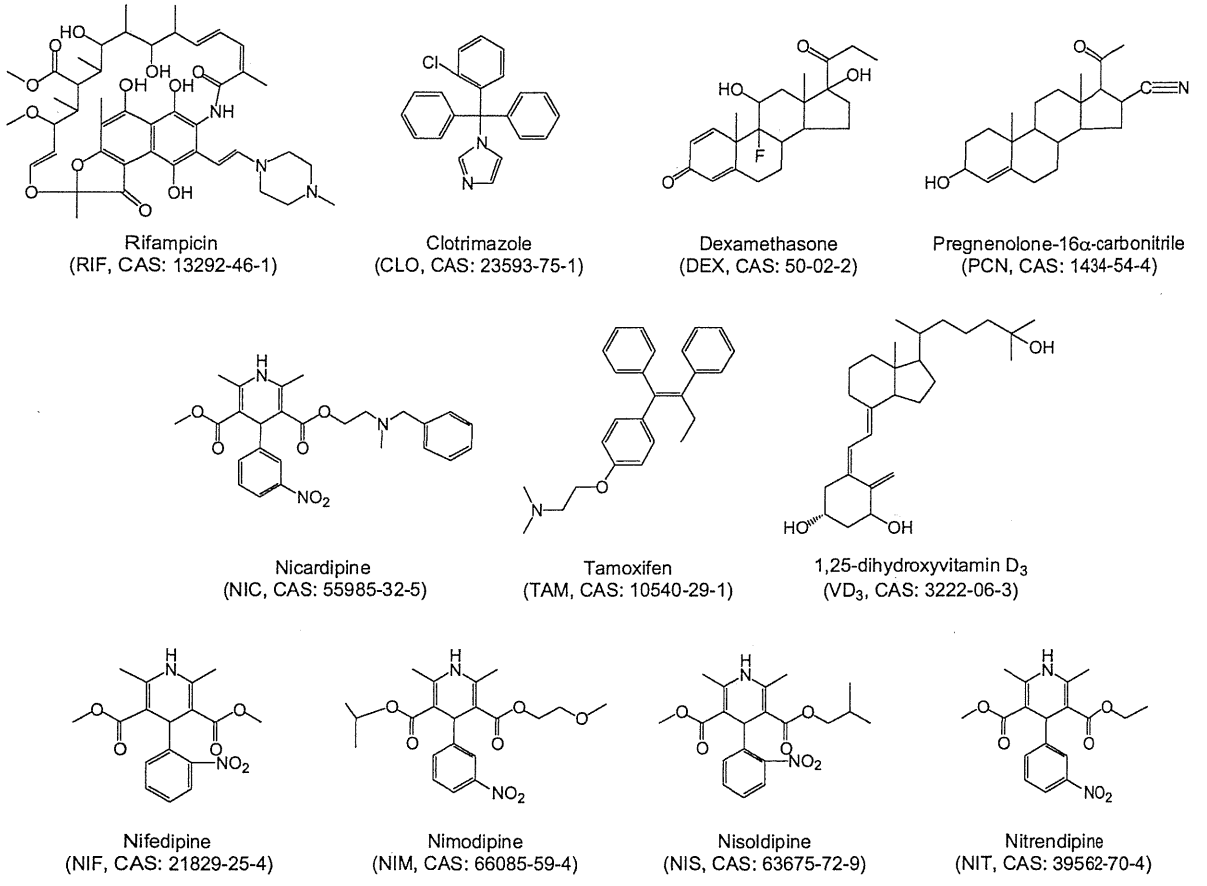

Fig. 1. Structures of Chemicals Used in This Study

luciferase gene and the promoter region (−362 to +53) and enhancer region (−7839 to −7208) of human *CYP3A4* gene was prepared using a previously reported method[16] with slight modifications.

In this study, human genomic DNA (Batch number; M00021571, Novagen, WI, U.S.A.) was used as a template for the amplification of the promoter/enhancer regions by polymerase chain reaction (PCR). A luciferase reporter plasmid, p3A4-hPXRE-Luc, was constructed through five steps as follows: (1) The promoter fragment A (−362 to +53) containing an ER-6 motif was prepared by *Bgl*II and *Bam*HI digestion of the promoter region (−1084 to +53), which was amplified by PCR with a primer set: forward sequence (bases −1085 to −1065, 5′-TCA TTG CTG GCT GAG GTG GTT-3′) and reverse sequence (bases +29 to +53, 5′-CAT GGA TCC TGT TGC TCT TTG CTG GGC TAT GTG C-3′), which has an engineered *Bam*HI digestion site, (2) The plasmid (p3A4-Luc) was constructed by insertion of the promoter fragment A into the *Bgl*II site of the PicaGene Basic Vector 2 (pGV-B2, NipponGene, Tokyo, Japan), (3) The enhancer fragment B (−7836 to −7208) containing dNR-1 and dNR-2 was prepared by PCR with a primer set: forward sequence (bases −7839 to −7810, 5′-GAA GAT CTA TTC TAG AGA GAT GGT TCA TTC CTT TCA-3′), which has an engineered *Bgl*II digestion site, and reverse sequence (bases −7208 to −7235, 5′-TCT CGT CAA CAG GTT AAA GGA GAA TGG T-3′), (4) The plasmid (hPXRE-pGEM-T) was prepared by insertion of the enhancer fragment B into the pGEM-T easy vector (Promega, Madison, MI, U.S.A.) containing a *Bam*HI site by the TA-cloning method, and (5) p3A4-hPXRE-Luc was prepared by insertion of the *Bam*HI–*Bgl*II digested hPXRE-pGEM-T fragment, containing enhancer fragment B, into the *Bgl*II site of p3A4-Luc. The obtained p3A4-hPXRE-Luc plasmid was used for the establishment of the cell line applicable to the hPXR-based chemically activated luciferase expression (CALUX) assay.

Construction of hPXR Expression Plasmid The full-length coding region of the human *PXR* gene was amplified from cDNA of a human hepatocellular carcinoma cell line, HepG2, by PCR with a primer set: forward sequence, 5′-GCC GCC ACC ATG GAG GTG AGA CCC AAA GAA AGC-3′; reverse sequence, 5′-AGC CGC TCA GCT ACC TGT GAT GCC GAA CAA-3′. An hPXR expression plasmid was prepared by the insertion of the full-length hPXR cDNA into the pTARGET Mammalian Expression vector (Promega) according to the manufacturer's instructions.

Establishment of a Cell Line for the hPXR-Based Reporter Gene Assay The reporter plasmid, p3A4-hPXRE-Luc, and the hPXR expression plasmid were co-transfected into HepG2 cells using Lipofectamine reagent (Life Technologies, Carlsbad, CA, U.S.A.) in Opti-MEM-I Reduced Serum Media (Life Technologies) for 24 h. After the co-transfection, a portion (10^4 cells/10 mL culture medium) of cell suspension was seeded in 100-mm culture dishes (Corning, Corning, NY, U.S.A.) and then cultured in Dulbecco's modified Eagle's medium (DMEM, Nissui, Tokyo, Japan) supplemented with 5% fetal calf serum and G418 (400 μg/mL medium) for

2 weeks. The G418-resistant cells were selected and further cloned. Consequently, eight clones (HPLs-A3, A7, A11, A12, A13, A14, A17 and A18) expressing hPXR and luciferase were obtained.

Luciferase Assay Luciferase assays were performed as previously described.[17,18] In brief, each HPL clone (5×10^4 cells/well) was pre-cultured for 48 h in a 24-well plate (Corning) and further incubated for the indicated times after addition of each test chemical to the culture medium. After incubation, cells were treated with 100 μL of 1×Reporter Lysis Buffer (Promega) for 15 min at room temperature, frozen at −80°C for 30 min and defrosted at room temperature. A portion (10 μL) of the resultant cell lysates was mixed with 50 μL of PicaGene Luminescence Reagent (Toyo-INK, Tokyo, Japan), and the amount of the luminescence product formed was immediately measured with a Luminescencer-PSN (ATTO, Tokyo, Japan). The amount of protein in cell lysates was measured using a bicinchoninic acid (BCA)-protein Assay Kit (Thermo Fisher Scientific, Rockford, IL, U.S.A.). Luciferase activity was represented as a luminescence unit per mg protein.

Clone HPL-A3 showed the greatest ability to induce chemical-mediated luciferase activity among the clones examined. Therefore, HPL-A3 was used for further experiments.

Gene Expression of CYP3A4 and Its Positive Transcriptional Regulators Constitutive gene expression levels of the positive transcriptional nuclear receptors (PXR, VDR, and CAR) of the *CYP3A4* gene and of their partner protein, retinoid X receptor α (RXRα), were determined by reverse transcription (RT)-PCR method[17,18] with the appropriate primer

Table 1. The Primer Sets and Amplification Protocols Used in This Study

Target gene	Primer set	Reaction condition			Cycle	Reference
		Denaturation	Annealing	Elongation		
Conventional PCR						
PXR	5′-TTG TTC GGC ATC ACA GGT AG-3′ (forward)	95°C, 30 s	60°C, 30 s	72°C, 60 s	25	(19)
	5′-CTT GCC TCT CTG ATG GTC CT-3′ (reverse)					
CAR	5′-GCA GCT GTG GAA ATC TGT CA-3′ (forward)	95°C, 30 s	60°C, 30 s	72°C, 60 s	35	(20)
	5′-CAG GTC GGT CAG GAG AGA AG-3′ (reverse)					
VDR	5′-CTC TTC AGA CAT GAT GGA CTC G-3′ (forward)	95°C, 30 s	60°C, 30 s	72°C, 60 s	28	(21)
	5′-GGA TGC TGT AAC TGA CCA GG-3′ (reverse)					
RXRα	5′-AGC TTG TGT CCA AGA TGC G-3′ (forward)	95°C, 30 s	60°C, 30 s	72°C, 60 s	25	(21)
	5′-ACT TGT GCT TGC AGT AGG CC-3′ (reverse)					
GAPDH	5′-TGT TGC CAT CAA TGA CCC CTT-3′ (forward)	95°C, 30 s	60°C, 30 s	72°C, 60 s	18	(22)
	5′-AGC ATC GCC CCA CTT GAT TTT G-3′ (reverse)					
Real-time PCR						
CYP3A4	5′-ATA AGT AAG GAA AGT AGT GAT GGC TCT CA-3′ (forward)	95°C, 30 s	60°C, 30 s	72°C, 60 s	40	(23)
	5′-TCA AAC ATA CAA AAG CCC TTA TGG TA-3′ (reverse)					
GAPDH	5′-TGT TGC CAT CAA TGA CCC CTT-3′ (forward)	95°C, 30 s	60°C, 30 s	72°C, 60 s	40	(22)
	5′-AGC ATC GCC CCA CTT GAT TTT G-3′ (reverse)					

sets.[19–23] The primer sets and amplification protocol used are shown in Table 1.

In brief, HPL-A3 or its parent cell line, HepG2, was cultured for 48 h in a 60-mm dish (Corning) (5×10^5 cells/dish). Total RNA was then isolated from the cells using Isogen (NipponGene). A portion (4 μg) of the prepared total RNA was converted to cDNA in an RT-reaction mixture (20 μL) containing Moloney Murine Leukemia Virus Reverse Transcriptase (Life Technologies) and Random Hexamers (Life Technologies). PCR was performed in a reaction mixture (25 μL) containing the prepared cDNA (equivalent to 32 ng of total RNA), the corresponding primer sets (each 12.5 pmol), and AmpliTaq Gold (0.625 units, Life Technologies) with a GeneAmp PCR system model 9600 (Life Technologies). The PCR products were separated by electrophoresis on a 2% agarose gel and visualized by ethidium bromide staining under UV light.

To determine chemical-altered *CYP3A4* expression, real-time PCR analysis was performed using an Applied Biosystems 7300 (Life Technologies) in 25 μL of reaction mixture containing the prepared cDNA (equivalent to 32 ng of total RNA), 12.5 μL of the Power SYBR Green PCR Master Mix (Life Technologies), the corresponding primer sets (each 12.5 pmol). After the reaction, dissociation curve analysis was carried out to confirm the amplification of a single PCR product. The amounts of CYP3A4 and glyceraldehyde-3-phosphate dehydrogenase (GAPDH) mRNAs were assessed by the relative standard curve method. *CYP3A4* and *GAPDH* fragments, obtained by conventional PCR with the corresponding primer sets (Table 1), were purified using a Qiaquick PCR Purification Kit (QIAEN, Valencia, CA, U.S.A.) and used as standard cDNAs. The level of CYP3A4 mRNA was normalized to that of GAPDH, an internal control.

Chemical-Mediated Induction of CYP3A Enzyme Activity The total activity of CYP3A subfamily enzymes was determined using a P450-Glo™ CYP3A4 Biochemical and Cell-Based Assay (Promega), as described in the instruction manual. In brief, HPL-A3 cells (10^4 cells/well) were pre-cultured for 48 h in a 96-well plate (Corning) and further treated with a chemical for the indicated times. After chemical treatment, cells were cultured for 4 h in serum-free DMEM containing Luciferin-PFBE (50 μM), a substrate of CYP3A subfamily enzymes (including CYP3A4, CYP3A5, and CYP3A7).[24] Thereafter, a portion (50 μL) of the culture supernatant was mixed with an equal volume of Luciferin Detection Reagent, and the mixture was incubated at room temperature for 20 min under light shielding. The amount of luciferin formed was measured using a Luminescencer-PSN. In addition, the protein contents of cell lysates were measured with a BCA-protein Assay Kit. The CYP3A enzyme activity was represented as a luminescence unit per mg protein.

Statistics Statistically significant differences between control group (treatment with a vehicle alone) and each chemical-treated group were assessed using Student's *t*-test. Time- and concentration-dependent effects were analyzed using one-way analysis of variance (ANOVA) and Dunnett's *post hoc* test. Furthermore, the correlation between two parameters was evaluated by regression analysis. These analyses were performed using ystat2002, a Microsoft Excel-based Statistical Program (Igaku Tosho Shuppan, Tokyo, Japan).

RESULTS

Selection of a Stable Cell Clone Applicable to hPXR-Based CALUX Assays G418-resistant cells were selected from HepG2 cells co-transfected with the reporter plasmid, p3A4-hPXRE-Luc, and the hPXR expression vector and further cloned. From 19 G418-resistant clones obtained, eight clones (HPLs-A3, A7, A11, A12, A13, A14, A17 and A18) that stably expressed luciferase were selected using the CALUX assay with RIF (10 μM), a representative hPXR activator. The concentration of RIF used was determined on the basis of previously reported data.[12,14] Clone HPL-A3 showed the greatest response to the RIF-mediated CALUX induction among the eight clones examined, although the other clones examined, with the exception of two clones (HPL-A14 and HPL-A18), showed moderate responses (Table 2). Therefore, HPL-A3 was selected and used for further experiments.

Time- and Concentration-Dependent Changes in the RIF-Mediated Induction of CALUX HPL-A3 was treated with RIF (10 μM), and the induced luciferase activities were measured at the indicated times. The luciferase activity increased in a time-dependent fashion up to 24 h after RIF-treatment and thereafter gradually decreased (Fig. 2A). Therefore, the reaction time was fixed at 24 h, and the concentration-effect of RIF on the induction of luciferase was further examined. RIF-mediated increases in luciferase activity occurred in a concentration-dependent fashion up to 100 μM (Fig. 2B).

RIF-Mediated Induction of CYP3A Subfamily Enzymes We first examined the induction of CYP3A enzyme activity according to the CYP3A4 p450-Glo™ Biochemical and Cell-Based Assay. The constitutive CYP3A activity in HPL-A3 was 0.107±0.036 RLU/μg protein, while in its parental cell line, HepG2, no CYP3A activity was detected. The time-dependent change in enzyme activity after treatment of HPL-A3 with RIF (10 μM) was then examined. The RIF-mediated increase in enzyme activity occurred in a time-dependent fashion up to 48 h, and the increased level at 48 h was maintained for up to 96 h (Fig. 3A). Considering such time-dependent induction, the concentration-effect of RIF was further assessed at 24 h. The RIF-mediated increase in CYP3A enzyme activity occurred in a concentration-dependent fashion up to 30 μM (Fig. 3B), while

Table 2. RIF-Mediated Induction of CALUX Activity in the Established Clones

Clone	Luciferase activity (luminescence unit/mg protein)		Induction ratio (RIF/CONT)
	CONT	10 μM RIF	
HPL-A3	4171±152	66958±2390**	16.05
HPL-A7	159186±1369	533185±8035**	3.35
HPL-A11	371±38	1020±45**	2.75
HPL-A12	275±17	1340±187**	4.87
HPL-A13	32895±2164	149212±7809**	4.54
HPL-A14	7844±6307	7743±3278	0.99
HPL-A17	105±2	121±5*	1.16
HPL-A18	107±11	118±5	1.10

The eight G418-resistant HepG2 clones, which stably express both PXR and luciferase, were treated with RIF or vehicle alone (CONT, 0.1% DMSO) for 24 h. Total cell lysates were prepared and used for the CALUX assay. The values represent the mean±S.E. in vehicle- and RIF-treated groups (n=3), respectively. *,** Significant differences from the corresponding vehicle-treated groups were assayed by Student's *t*-test; * $p<0.05$, ** $p<0.01$.

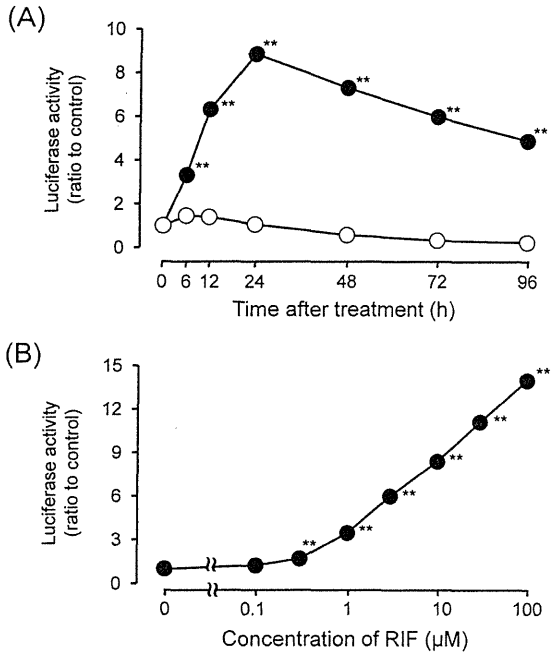

Fig. 2. Time–Course or Dose-Dependent Changes in CALUX in HPL-A3 after Treatment with RIF

HPL-A3 cells were treated with RIF (10 μM) or with vehicle alone (0.1% DMSO) for the indicated times (A) or were treated with RIF at the indicated concentrations for 24 h (B), and total cell lysates were used for the CALUX assay. The luciferase activity was measured as described in the Materials and Methods, and the data are represented as a ratio relative to corresponding controls. Solid and open circles represent the mean in RIF- and vehicle-treated groups, respectively (n=4), and the bars show their standard errors. **Significant differences from the corresponding controls assayed by ANOVA and Dunnett's test; **p<0.01.

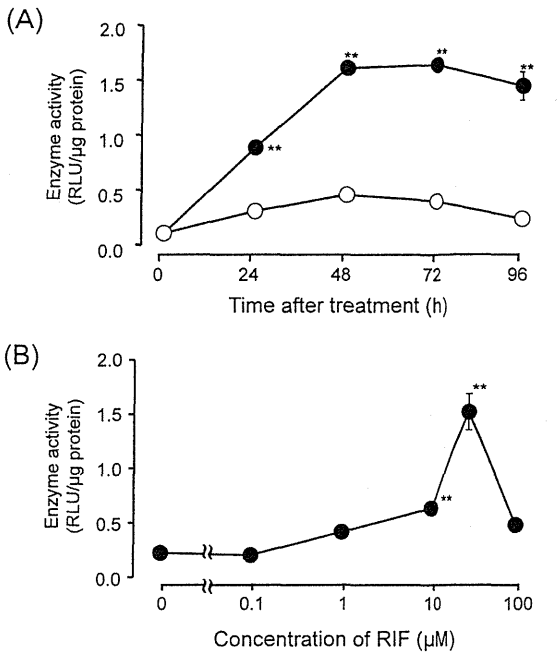

Fig. 3. Time–Course or Dose-Dependent Changes in the Activity of CYP3A Subfamily Enzymes in HPL-A3 after Treatment with RIF

HPL-A3 cells were treated with RIF (10 μM) or with vehicle alone (0.1% DMSO) for the indicated times (A) or were treated with RIF at various concentrations for 24 h (B). CYP3A enzyme activity was assessed by p450-Glo CYP3A4 assays, and the data are represented as a ratio relative to the control (treated with vehicle alone). Solid and open circles represent the mean in RIF- and vehicle-treated groups, respectively (n=3), and the bars show their standard errors. **Significant differences from the corresponding controls assayed by ANOVA and Dunnett's test; **p<0.01.

no such significant increase was observed at 100 μM.

The constitutive level of *CYP3A4* expression was measured by a real-time RT-PCR method. The constitutive *CYP3A4* expression level in HPL-A3 was 1.6-fold higher than in HepG2. Subsequently, the time-dependent change in the level of *CYP3A4* expression after treatment with RIF (10 μM) was examined. The expression level was increased in a time-dependent fashion up to 24 h (Fig. 4A). The increased level was maintained for up to 48 h and thereafter gradually decreased. *CYP3A4* expression at 24 h was about 5-fold higher than the corresponding control level. In addition, 24 h after the RIF treatment, the expression levels of *CYP3A5* and *CYP3A7* were likewise increased 3–3.5-fold compared with the corresponding control levels (data not shown). A concentration-effect of RIF on expression of *CYP3A4* was further examined at 24 h after RIF-treatment. *CYP3A4* expression was increased in a concentration-dependent fashion up to 100 μM (Fig. 4B). Moreover, there was a significantly positive correlation between the CALUX (luciferase activity) and the gene expression of CYP3A4 (Fig. 4C).

Usefulness of HPL-A3 for Screening Human CYP3A Inducers It has been reported that species specificity in the induction of CYP3A subfamily enzymes by xenobiotics is likely to be a consequence of differences at the level of PXR activation.[25,26] Therefore, we comparatively examined the effects of the human and/or rodent PXR ligands on the inductions of CALUX and CYP3A4 mRNA in HPL-A3. In this experiment, human PXR activators (RIF and CLO), human/mouse/rat PXR activators (TAM and NIC), and mouse/rat PXR activators (DEX and PCN) were used as representative species-selective PXR activators.[27–30] The working concentration of each chemical (10 μM) was determined on the basis of previously reported data.[14,28,30]

Treatments of HPL-A3 with RIF, CLO, TAM and NIC for 24 h resulted in significant increases in CALUX, represented as luciferase activity (Fig. 5A). On the other hand, no significant increases by DEX and PCN were observed. Significant increases in the level of *CYP3A4* expression was likewise observed in HPL-A3 treated with RIF, CLO, TAM or NIC, but not with DEX and PCN (Fig. 5B). Furthermore, there were significantly positive correlations between CALUX and the level of *CYP3A4* expression in the chemical-treated HPL-A3 cells (Fig. 5C).

Induction of CALUX by Calcium Channel Blockers We have previously reported that several dihydropyridine calcium channel blockers (CCBs), especially NIC, showed abilities to induce hepatic CYP3A subfamily enzymes in rats and mice.[31–33] Therefore, the effects on CALUX of CCBs, such as NIC, NIF, NIM, NIT or NIS, were assessed using HPL-A3 cells. The CALUX assay was performed 24 h after incubation with each CCB. The increases in CALUX in response to all the CCBs used occurred in a concentration-dependent fashion (Fig. 6). In addition, NIS showed cytocidal effects on HPL-A3 cells at concentrations of more than 10 μM. When the effects on the induction of CALUX were compared among CCBs at 3 μM, they were active in the following order: NIM>NIC, NIT>NIS, NIF.

Gene Expression of Positive Transcriptional Regulators

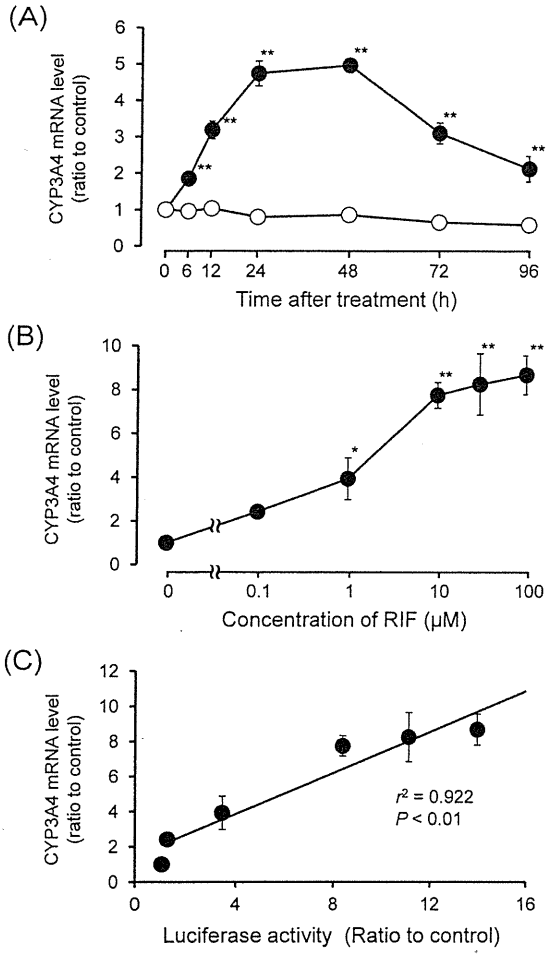

Fig. 4. Time–Course or Dose-Dependent Changes in the Level of CYP3A4 mRNA in HPL-A3 after Treatment with RIF

HPL-A3 cells were treated with RIF (10 μM) or with a vehicle alone (0.1% DMSO) for the indicated times (A) or were treated with RIF at the indicated concentrations for 24 h (B), and the total RNA from the cells was used for real-time RT-PCR analysis. The level of CYP3A4 mRNA was normalized to that of GAPDH mRNA and represented as a ratio relative to the corresponding controls. The correlations between luciferase activities (as shown in Fig. 2B) and the levels of CYP3A4 mRNA after the treatment with RIF at various concentrations for 24 h were assessed by regression analysis (C). Solid and open circles represent the means of RIF- and vehicle-treated groups (n=3), respectively, and the bars show their standard errors. ***Significant differences from the corresponding controls assayed by ANOVA and Dunnett's test; *p<0.05, **p<0.01.

of the *CYP3A4* Gene It has been reported that not only PXR but also CAR and VDR are associated with chemical-mediated activation of *CYP3A4* expression.[8,9] Therefore, we examined the constitutive gene expression levels of PXR, CAR, and VDR in HPL-A3 cells, and their levels were compared with those in HepG2. Likewise, the gene expression levels of RXRα, a partner protein for PXR, CAR, and VDR, were comparatively examined. As expected, the constitutive expression level of *PXR* in HPL-A3, which is transfected with an hPXR expression vector, was higher than in the HepG2 parental cell line (Fig. 7). On the other hand, only low level expression of *CAR* was observed in either HPL-A3 or HepG2. No clear difference in the expression level of *RXRα* between HPL-A3 and HepG2 was observed. The expression level of *VDR* was surprisingly clearly increased in HPL-A3 compared with HepG2.

VD_3-Mediated Induction of CALUX and *CYP3A4* Expression Since HPL-A3 was predicted to express VDR, the

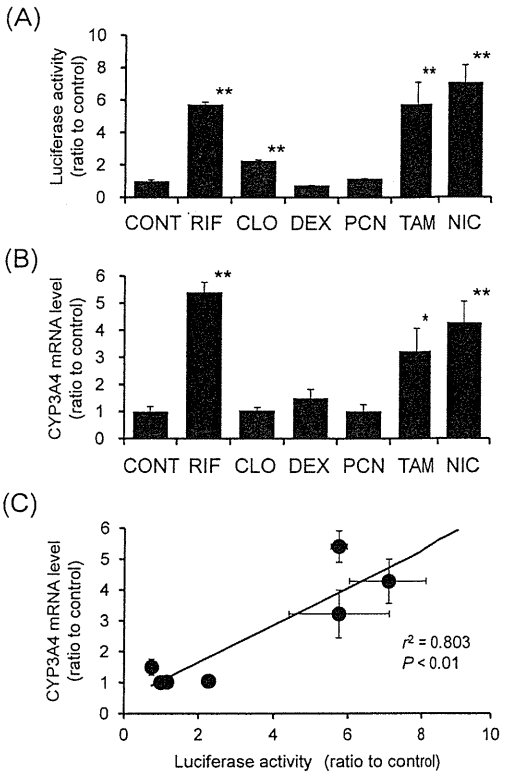

Fig. 5. Effects of Various Chemicals on the Induction of CALUX and CYP3A4 mRNA in HPL-A3

HPL-A3 cells were treated with each chemical (10 μM) for 24 h. Total cell lysates and total RNA were used for CALUX assay and real-time RT-PCR analysis, respectively. The luciferase activity is represented as a ratio relative to the control (treated with vehicle alone) (A). The level of CYP3A4 mRNA was normalized to that of GAPDH mRNA and represented as a ratio relative to the corresponding controls (B). The correlations between luciferase activities and the levels of CYP3A4 mRNA after the chemical-treatment for 24 h were assessed by regression analysis (C). ***Significant differences from the corresponding controls assayed by ANOVA and Dunnett's test; *p<0.05, **p<0.01.

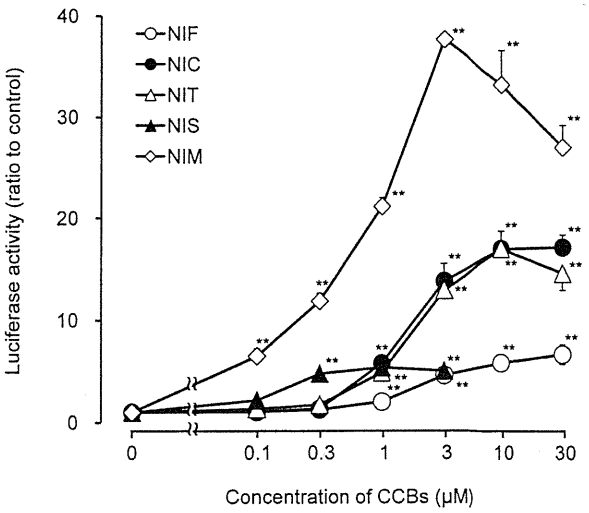

Fig. 6. Dose-Dependent Changes in CALUX in HPL-A3 Cells after Treatment with Calcium Channel Blockers

HPL-A3 cells were treated with a calcium channel blocker (NIC, NIF, NIM, NIT or NIS) at the indicated concentrations for 24 h, and total cell lysates were used for the CALUX assay. The luciferase activity is shown as a ratio relative to the control (treated with vehicle alone). The values represent the mean in each group (n=3), and the bars show their standard errors. **Significant differences from the corresponding controls assayed by ANOVA and Dunnett's test; **p<0.01.

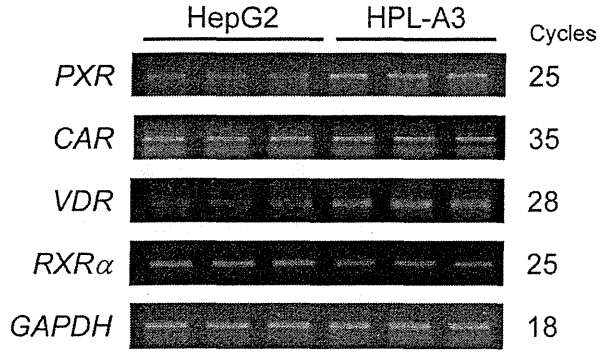

Fig. 7. Gene Expression of Positive Transcriptional Regulators of the *CYP3A4* Gene in HPL-A3 Cells and the Parental Cell Line, HepG2

Total RNA was prepared from HPL-A3 or HepG2 cells and used for conventional RT-PCR analyses of PXR, VDR, CAR and RXRα mRNAs. *GAPDH* was used as an internal standard. The PCR products were separated by electrophoresis on a 2% agarose gel and visualized by ethidium bromide staining under UV light.

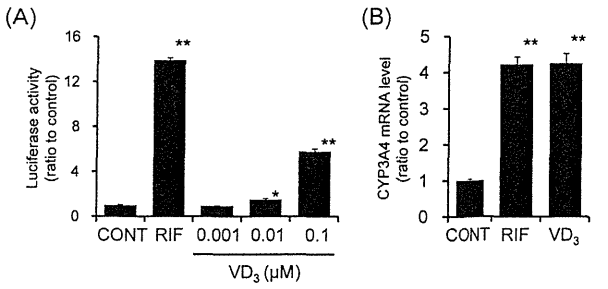

Fig. 8. Effects of VD_3 on the Induction of CALUX and CYP3A4 mRNA in HPL-A3

HPL-A3 cells were treated with VD_3 at the indicated concentrations for 24 h, and their total cell lysates were used for the CALUX assay. RIF (10 μM) was used as a positive control. The luciferase activity is represented as a ratio relative to the control (treated with vehicle alone) (A). The real-time RT-PCR analysis for CYP3A4 mRNA was performed using cells treated with VD_3 (0.1 μM) or RIF (10 μM) for 24 h (B). The level of CYP3A4 mRNA was normalized to that of GAPDH mRNA and represented as a ratio relative to the corresponding controls. The solid columns represent the mean in each group (n=3), and the bars show their standard errors. ***Significant differences from the corresponding controls assayed by ANOVA and Dunnett's test; *$p<0.05$, **$p<0.01$.

effects of VD_3, a VDR ligand, on the induction of CALUX and CYP3A4 mRNA were examined. The working concentration (0.1 μM) of VD_3 was determined on the basis of previously reported data.[8,34]

After VD_3-treatment, luciferase activity was increased in a time-dependent fashion up to 24 h (data not shown). Therefore, the reaction time was fixed at 24 h, and the concentration-effect of VD_3 on the induction of CALUX was examined. CALUX induction occurred in a concentration-dependent fashion in the range of 0.01–0.1 μM (Fig. 8A). In addition, a significant increase in *CYP3A4* expression was confirmed in HPL-A3 treated with VD_3 (0.1 μM) for 24 h (Fig. 8B).

DISCUSSION

In the present study, we established an HPL-A3 cell line by co-transfection of the p3A4-hPXRE-Luc reporter plasmid and an hPXR expression plasmid into HepG2 cells, and the applicability of the cell line to the hPXR-based CALUX assay was first assessed using RIF, a representative hPXR activator. The time- and concentration-dependent inductions of CALUX and *CYP3A4* expression by RIF were clearly observed in HPL-A3, and significantly positive correlation between CALUX (luciferase activity) and *CYP3A4* expression was also observed. In addition, RIF-mediated induction of CYP3A enzyme activity occurred in a concentration-dependent fashion up to 30 μM, but at a higher concentration (100 μM), the increased activity was reduced. These phenomena can be attributed to the biochemical properties of RIF; it has the ability not only to induce CYP3A subfamily enzymes[35] but also to inhibit the activities of several CYP enzymes, including CYP3A4.[36]

CALUX in HPL-A3 was further increased not only by hPXR-selective activators (RIF and CLO) but also by human/mouse/rat PXR activators (TAM and NIC), while no such significant increases by mouse/rat PXR activators (DEX and PCN) were observed. These results suggest that HPL-A3 is adaptable for use in hPXR-based reporter gene assays.

We have previously reported that CCBs, such as NIC, NIF, NIM, NIT and NIS, show abilities to induce hepatic CYP3A subfamily enzymes in rats.[37] These CCBs are also known to have affinity to hPXR and to show the ability to activate hPXR-based reporter genes.[27,38–40] Therefore, we examined the capacities of NIC, NIF, NIM, NIT and NIS for hPXR activation using HPL-A3, and confirmed that all the CCBs used act as hPXR activators. Furthermore, we demonstrated that they were active in the following order: NIM>NIC, NIT>NIS, NIF. This order was similar to that in a previous report on the induction of hepatic *CYP3A1* in rats.[37]

To further understand the mechanisms for the xenobiotic-mediated induction of CALUX and *CYP3A4* expression in HPL-A3, we examined the gene expression of transcriptional factors, such as PXR, CAR, VDR and their partner protein (RXRα), that are involved in the regulation of *CYP3A4* expression. As expected, the expression level of *PXR* was significantly increased in HPL-A3, which is transfected with an hPXR expression vector, compared with that in the HepG2 parental cell line. The gene expression level of VDR was likewise increased. However, the mechanism for the increase in gene expression of VDR remains unclear, although the increase might be dependent on the insertion sites of the hPXR expression vector and/or the reporter plasmid p3A4-PXRE-Luc in the genome of host cells. In addition, no clear changes in the expression levels of *CAR* or *RXRα* by the insertion of the expression vector and reporter plasmid were observed in HPL-A3.

Because a high level of *VDR* expression is predicted in HPL-A3, we further examined whether VD_3, a representative ligand of hVDR, can induce CALUX and CYP3A4 mRNA in HPL-A3 cells, and we indeed demonstrated VD_3-mediated inductions. Although the expression level of VDR is not especially high in human hepatocytes,[41,42] it has been reported that the activation of VDR led to modifications in the expression of hepatic CYPs, such as CYP3A4,[8] CYP7A1 and CYP24A1,[10] and to altered hepatic lipid metabolism.[43] The previous and present findings therefore suggest that HPL-A3 is a useful tool for the screening of hVDR activators/inhibitors and for the analysis of hVDR function in the liver.

In conclusion, we have established an HPL-A3 cell line, which is a useful tool for the screening of not only human CYP3A inducers but also the activators/inhibitors of CYP3A transcription factors, such as hPXR and hVDR. Studies on the altered expression of CYP3A subfamily enzymes, especially

CYP3A4, by xenobiotics such as drugs are important for understanding the therapeutic/toxic effects of drugs and environmental chemicals. Therefore, the established HPL-A3 cell line will greatly contribute to the development of these studies.

Acknowledgments We thank Ms. K. Yabe and Mr. S. Hirai (Department of Molecular Toxicology, School of Pharmaceutical Sciences, University of Shizuoka) for assistance with experiments in this study. This work was supported in part by a Research Grant-in-Aid from the Ministry of Health, Labour and Welfare of Japan (M.D.).

REFERENCES

1) Danielson PB. The cytochrome P450 superfamily: biochemistry, evolution and drug metabolism in humans. *Curr. Drug Metab.*, **3**, 561–597 (2002).
2) Zhou SF. Drugs behave as substrates, inhibitors and inducers of human cytochrome P450 3A4. *Curr. Drug Metab.*, **9**, 310–322 (2008).
3) Tachibana T, Kato M, Takano J, Sugiyama Y. Predicting drug–drug interactions involving the inhibition of intestinal CYP3A4 and P-glycoprotein. *Curr. Drug Metab.*, **11**, 762–777 (2010).
4) Donato MT, Lahoz A, Castell JV, Gómez-Lechón MJ. Cell lines: a tool for *in vitro* drug metabolism studies. *Curr. Drug Metab.*, **9**, 1–11 (2008).
5) Aninat C, Piton A, Glaise D, Le Charpentier T, Langouët S, Morel F, Guguen-Guillouzo C, Guillouzo A. Expression of cytochromes P450, conjugating enzymes and nuclear receptors in human hepatoma HepaRG cells. *Drug Metab. Dispos.*, **34**, 75–83 (2006).
6) Kliewer SA, Moore JT, Wade L, Staudinger JL, Watson MA, Jones SA, McKee DD, Oliver BB, Willson TM, Zetterström RH, Perlmann T, Lehmann JM. An orphan nuclear receptor activated by pregnanes defines a novel steroid signaling pathway. *Cell*, **92**, 73–82 (1998).
7) Lehmann JM, McKee DD, Watson MA, Willson TM, Moore JT, Kliewer SA. The human orphan nuclear receptor PXR is activated by compounds that regulate CYP3A4 gene expression and cause drug interactions. *J. Clin. Invest.*, **102**, 1016–1023 (1998).
8) Drocourt L, Ourlin JC, Pascussi JM, Maurel P, Vilarem MJ. Expression of CYP3A4, CYP2B6, and CYP2C9 is regulated by the vitamin D receptor pathway in primary human hepatocytes. *J. Biol. Chem.*, **277**, 25125–25132 (2002).
9) Moore LB, Parks DJ, Jones SA, Bledsoe RK, Consler TG, Stimmel JB, Goodwin B, Liddle C, Blanchard SG, Willson TM, Collins JL, Kliewer SA. Orphan nuclear receptors constitutive androstane receptor and pregnane X receptor share xenobiotic and steroid ligands. *J. Biol. Chem.*, **275**, 15122–15127 (2000).
10) Han S, Chiang JYL. Mechanism of vitamin D receptor inhibition of cholesterol 7α-hydroxylase gene transcription in human hepatocytes. *Drug Metab. Dispos.*, **37**, 469–478 (2009).
11) Raucy J, Warfe L, Yueh MF, Allen SW. A cell-based reporter gene assay for determining induction of CYP3A4 in a high-volume system. *J. Pharmacol. Exp. Ther.*, **303**, 412–423 (2002).
12) Lemaire G, de Sousa G, Rahmani R. A PXR reporter gene assay in a stable cell culture system: CYP3A4 and CYP2B6 induction by pesticides. *Biochem. Pharmacol.*, **68**, 2347–2358 (2004).
13) Yueh MF, Kawahara M, Raucy J. High volume bioassays to assess CYP3A4-mediated drug interactions: induction and inhibition in a single cell line. *Drug Metab. Dispos.*, **33**, 38–48 (2005).
14) Lemaire G, Mnif W, Pascussi JM, Pillon A, Rabenoelina F, Fenet H, Gomez E, Casellas C, Nicolas JC, Cavaillès V, Duchesne MJ, Balaguer P. Identification of new human pregnane X receptor ligands among pesticides using a stable reporter cell system. *Toxicol. Sci.*, **91**, 501–509 (2006).
15) Noracharttiyapot W, Nagai Y, Matsubara T, Miyata M, Shimada M, Nagata K, Yamazoe Y. Construction of several human-derived stable cell lines displaying distinct profiles of CYP3A4 induction. *Drug Metab. Pharmacokinet.*, **21**, 99–108 (2006).
16) Goodwin B, Hodgson E, Liddle C. The orphan human pregnane X receptor mediates the transcriptional activation of CYP3A4 by rifampicin through a distal enhancer module. *Mol. Pharmacol.*, **56**, 1329–1339 (1999).
17) Sekimoto M, Iwamoto M, Miyajima S, Nemoto K, Degawa M. Establishment of a rat hepatic cell line, KanR2-XL8, for a reporter gene assay of aryl hydrocarbon receptor ligands. *J. Health Sci.*, **50**, 530–536 (2004).
18) Sekimoto M, Kawamagari H, Nakatani S, Nemoto K, Degawa M. Establishment of a human hepatoma cell line HepG2-A10 for a reporter gene assay of arylhydrocarbon receptor activators. *Genes Environ.*, **29**, 11–16 (2007).
19) Dotzlaw H, Leygue E, Watson P, Murphy LC. The human orphan receptor PXR messenger RNA is expressed in both normal and neoplastic breast tissue. *Clin. Cancer Res.*, **5**, 2103–2107 (1999).
20) Malaplate-Armand C, Ferrari L, Masson C, Visvikis-Siest S, Lambert H, Batt AM. Down-regulation of astroglial CYP2C, glucocorticoid receptor and constitutive androstane receptor genes in response to cocaine in human U373 MG astrocytoma cells. *Toxicol. Lett.*, **159**, 203–211 (2005).
21) Matsubara T, Yoshinari K, Aoyama K, Sugawara M, Sekiya Y, Nagata K, Yamazoe Y. Role of vitamin D receptor in the lithocholic acid-mediated CYP3A induction *in vitro* and *in vivo*. *Drug Metab. Dispos.*, **36**, 2058–2063 (2008).
22) Tian W, Osawa M, Horiuchi H, Tomita Y. Expression of the prolactin-inducible protein (PIP/GCDFP15) gene in benign epithelium and adenocarcinoma of the prostate. *Cancer Sci.*, **95**, 491–495 (2004).
23) Zhuo X, Zheng N, Felix CA, Blair IA. Kinetics and regulation of cytochrome P450-mediated etoposide metabolism. *Drug Metab. Dispos.*, **32**, 993–1000 (2004).
24) Cali JJ, Ma D, Sobol M, Simpson DJ, Frackman S, Good TD, Daily WJ, Liu D. Luminogenic cytochrome P450 assays. *Expert Opin. Drug Metab. Toxicol.*, **2**, 629–645 (2006).
25) Jones SA, Moore LB, Shenk JL, Wisely GB, Hamilton GA, McKee DD, Tomkinson NC, LeCluyse EL, Lambert MH, Willson TM, Kliewer SA, Moore JT. The pregnane X receptor: a promiscuous xenobiotic receptor that has diverged during evolution. *Mol. Endocrinol.*, **14**, 27–39 (2000).
26) LeCluyse EL. Pregnane X receptor: molecular basis for species differences in CYP3A induction by xenobiotics. *Chem. Biol. Interact.*, **134**, 283–289 (2001).
27) Drocourt L, Pascussi JM, Assenat E, Fabre JM, Maurel P, Vilarem MJ. Calcium channel modulators of the dihydropyridine family are human pregnane X receptor activators and inducers of CYP3A, CYP2B, and CYP2C in human hepatocytes. *Drug Metab. Dispos.*, **29**, 1325–1331 (2001).
28) Vignati LA, Bogni A, Grossi P, Monshouwer M. A human and mouse pregnane X receptor reporter gene assay in combination with cytotoxicity measurements as a tool to evaluate species-specific CYP3A induction. *Toxicology*, **199**, 23–33 (2004).
29) Sane RS, Buckley DJ, Buckley AR, Nallani SC, Desai PB. Role of human pregnane X receptor in tamoxifen- and 4-hydroxytamoxifen-mediated CYP3A4 induction in primary human hepatocytes and LS174T cells. *Drug Metab. Dispos.*, **36**, 946–954 (2008).
30) Cui X, Thomas A, Gerlach V, White RE, Morrison RA, Cheng KC. Application and interpretation of hPXR screening data: Validation of reporter signal requirements for prediction of clinically relevant CYP3A4 inducers. *Biochem. Pharmacol.*, **76**, 680–689 (2008).
31) Konno Y, Nemoto K, Degawa M. Induction of hepatic cytochrome P450s responsible for the metabolism of xenobiotics by nicardipine and other calcium channel antagonists in the male rat. *Xenobiotica*, **33**, 119–129 (2003).
32) Konno Y, Sekimoto M, Nemoto K, Degawa M. Sex difference in

induction of hepatic CYP2B and CYP3A subfamily enzymes by nicardipine and nifedipine in rats. *Toxicol. Appl. Pharmacol.*, **196**, 20–28 (2004).
33) Konno Y, Sekimoto M, Nemoto K, Degawa M. Induction of hepatic Cyp2b and Cyp3a subfamily enzymes by nicardipine and nifedipine in mice. *Xenobiotica*, **34**, 607–618 (2004).
34) Khan AA, Chow ECY, van Loenen-Weemaes AMMA, Porte RJ, Pang KS, Groothuis GMM. Comparison of effects of VDR *versus* PXR, FXR and GR ligands on the regulation of CYP3A isozymes in rat and human intestine and liver. *Eur. J. Pharm. Sci.*, **37**, 115–125 (2009).
35) Gillum JG, Israel DS, Polk RE. Pharmacokinetic drug interactions with antimicrobial agents. *Clin. Pharmacokinet.*, **25**, 450–482 (1993).
36) Kajosaari LI, Laitila J, Neuvonen PJ, Backman JT. Metabolism of repaglinide by CYP2C8 and CYP3A4 *in vitro*: effect of fibrates and rifampicin. *Basic Clin. Pharmacol. Toxicol.*, **97**, 249–256 (2005).
37) Konno Y, Degawa M. Gene activations of CYP2B1 and CYP3A1 by dihydropyridine calcium channel antagonists in the rat liver: the structure–activity relationship. *Biol. Pharm. Bull.*, **27**, 903–905 (2004).
38) Pan Y, Li L, Kim G, Ekins S, Wang H, Swaan PW. Identification and validation of novel human pregnane X receptor activators among prescribed drugs *via* ligand-based virtual screening. *Drug Metab. Dispos.*, **39**, 337–344 (2011).
39) Shukla SJ, Sakamuru S, Huang R, Moeller TA, Shinn P, Vanleer D, Auld DS, Austin CP, Xia M. Identification of clinically used drugs that activate pregnane X receptors. *Drug Metab. Dispos.*, **39**, 151–159 (2011).
40) Xiao L, Nickbarg E, Wang W, Thomas A, Ziebell M, Prosise WW, Lesburg CA, Taremi SS, Gerlach VL, Le HV, Cheng KC. Evaluation of *in vitro* PXR-based assays and *in silico* modeling approaches for understanding the binding of a structurally diverse set of drugs to PXR. *Biochem. Pharmacol.*, **81**, 669–679 (2011).
41) Nishimura M, Naito S, Yokoi T. Tissue-specific mRNA expression profiles of human nuclear receptor subfamilies. *Drug Metab. Pharmacokinet.*, **19**, 135–149 (2004).
42) Bookout AL, Jeong Y, Downes M, Yu RT, Evans RM, Mangelsdorf DJ. Anatomical profiling of nuclear receptor expression reveals a hierarchical transcriptional network. *Cell*, **126**, 789–799 (2006).
43) Wang JH, Keisala T, Solakivi T, Minasyan A, Kalueff AV, Tuohimaa P. Serum cholesterol and expression of ApoAI, LXRβ and SREBP2 in vitamin D receptor knock-out mice. *J. Steroid Biochem. Mol. Biol.*, **113**, 222–226 (2009).